

UC Santa Cruz

UC Santa Cruz Previously Published Works

Title

Author Correction: Warming and cooling catalyse widespread temporal turnover in biodiversity

Permalink

<https://escholarship.org/uc/item/7m38c9v0>

Authors

Pinsky, Malin L
Hillebrand, Helmut
Chase, Jonathan M
[et al.](#)

Publication Date

2025

DOI

10.1038/s41586-025-08857-8

Copyright Information

This work is made available under the terms of a Creative Commons Attribution License, available at <https://creativecommons.org/licenses/by/4.0/>

Peer reviewed

Title: Warming and cooling catalyze widespread temporal turnover in biodiversity

Authors: Malin L. Pinsky^{1,2*}, Helmut Hillebrand³, Jonathan M. Chase^{4,5}, Laura H. Antão⁶, Myriam R. Hirt^{4,7}, Ulrich Brose^{4,7}, Michael T. Burrows⁸, Benoit Gauzens^{4,7}, Benjamin Rosenbaum^{4,7}, and Shane A. Blowes^{4,5}

Affiliations:

¹ Department of Ecology, Evolution, and Natural Resources, Rutgers University, New Brunswick, NJ 08901, USA

² Department of Ecology & Evolutionary Biology, University of California Santa Cruz, Santa Cruz, CA 95060, USA

³ Institute for Chemistry and Biology of Marine Environments (ICBM), University of Oldenburg, Wilhelmshaven, Germany

⁴ German Centre for Integrative Biodiversity Research (iDiv) Halle-Jena-Leipzig, Leipzig, Germany

⁵ Institute of Computer Science, Martin Luther University Halle-Wittenberg, Halle (Saale), Germany

⁶ Research Centre for Ecological Change, Faculty of Biological and Environmental Sciences, University of Helsinki, 00014 Helsinki, Finland

⁷ Institute of Biodiversity, Friedrich Schiller University Jena, Jena, Germany

⁸ Scottish Association for Marine Science, Oban, Argyll PA37 1QA, United Kingdom

* Corresponding author: Malin L. Pinsky, mpinsky@ucsc.edu

Summary paragraph:

Turnover in species composition through time is a dominant form of biodiversity change that has profound impacts on the functioning of ecological communities (1–4). Turnover rates differ dramatically among communities (4), but the drivers of this variation across taxa and realms remain unknown. Here, we analyze 42,255 time series of species composition from marine, terrestrial and freshwater assemblages and show that temporal rates of turnover were consistently faster in locations that experienced faster temperature change, including both warming and cooling. In addition, assemblages with limited access to microclimate refugia or that faced stronger human impacts on land were especially responsive to temperature change, with up to 48% of species replaced per decade. These results reveal a widespread signal of vulnerability to ongoing climate change and highlight which ecological communities are most sensitive, raising concerns about ecosystem integrity as climate change and other human impacts accelerate.

Main text:

One of the most prominent signatures of biodiversity change in the Anthropocene is the rapid change in species composition through time, hereafter referred to as temporal turnover (1, 2). Turnover occurs when some species increase their abundance or occupancy through time while others decline. Such temporal turnover has dramatic impacts on the structure and functioning of ecological communities (3) and can be rapid even while the number of species remains relatively unchanged (1, 2). However, the rates of temporal turnover differ substantially across locations, from little change over many decades in some communities to almost complete turnover within years in others (1, 4). The reasons for this variation across organism and ecosystem types remain unclear, in part because most previous research has focused on particular taxa or locations (5–9).

One possible explanation for this variation is that assemblages are exposed to differing rates of environmental change and have differing sensitivities to those changes (1, 4). Of the multiple environmental drivers that shape species distributions and abundance, temperature is particularly

important for biological processes across the tree of life (10). For example, changing temperatures have a strong influence on organismal physiology and species distributions (10, 11), and these effects differ systematically across taxa and between marine, terrestrial and freshwater realms (12–14). Systematic differences in temperature change and in species sensitivity to such changes may therefore help explain why some assemblages change composition quickly and others more slowly. Here, we i) tested the extent to which rates of temporal turnover increased with rates of temperature change using the largest compilation of biodiversity surveys through time available, and ii) explicitly evaluated which factors modified this relationship, including ecological realm, the degree of thermal habitat heterogeneity (i.e., availability of microclimates), and the extent of human impacts (e.g., land use and invasive species).

We compiled temporal turnover rates from 257,289 observations of species composition across 42,255 assemblage time series around the world covering a wide range of taxa from the BioTIME database (15) (see Methods, Fig. 1a and Extended Data Fig. 1). Following standard practice, we measured temporal turnover as the rate at which dissimilarity in species composition changed through time using the incidence-based Jaccard index, and specifically the component of dissimilarity that quantifies species replacement independent of changes in species richness (see Methods) (4, 16). Dissimilarity is bound to values between 0 (i.e., no change in composition) and 1 (i.e., complete turnover), and changes in turnover over time (i.e. turnover rate) are positive if compositional change accumulates over time. For example, birds in Sweden had a temporal turnover rate of 0.0046 per year (± 0.00017 standard error, Fig. 1d), meaning that 0.46% of species were replaced per year in this assemblage. Turnover rate can also be negative if composition becomes more similar to initial assemblages again (Extended Data Fig. 2f).

Across all studies, dissimilarity generally increased with time, yielding positive temporal turnover rates (Fig. 2a, median = 0.0082 per year [i.e., 0.82% per year] with a 95% bootstrap confidence interval of 0.0065 to 0.0095). The few studies with negative turnover rates mostly had shorter durations, where variation in estimated rates was highest ($n = 46$, Extended Data Fig. 2b). On average, assemblages experienced warming of 0.27 °C per decade on land and of 0.20 °C per decade in the ocean, but there was also large variation in the magnitude and direction of temperature change, and many assemblages experienced cooling (Fig. 1b, c). The rates of temperature change for these local time series were often faster than for global temperatures since the time series were shorter (median 8 year duration). Statistical challenges with this type of dataset include pseudoreplication within time series and studies, the non-linearity of species composition turnover, and the heteroskedasticity introduced by time series of differing lengths (17–19). Many statistical approaches produce high false positive error rates with datasets like this, but generalized linear mixed models (GLMMs) with ordered beta errors and environmental drivers as interaction effects kept false positive rates low (see Methods, conceptual diagrams in Fig. 1e and Extended Data Fig. 3, and Extended Data Fig. 2). We used this latter approach to evaluate the role of temperature change and other environmental drivers underpinning global variation in temporal turnover rates.

Temperature change and turnover rates

Rates of turnover were associated with the rate of local temperature change, such that higher turnover rates occurred with faster rates of temperature change. Models with a temperature change effect on turnover rate outperformed alternative models without this effect ($\chi^2 = 143$, $df = 9$, two-sided $p < 2.2 \times 10^{-16}$, likelihood ratio test against a GLMM without a temperature change effect on turnover rate, $n = 40,332$ time series, see Methods) or models that only considered differences among realms or taxonomic groups (Table 1, Fig. 2 and Extended Data Fig. 4a).

Up to 5.1% of the species in an assemblage on average were replaced each year where rates of temperature change were highest in the terrestrial realm, and up to 5.2% in freshwater and 3.2% in the ocean, though few locations experienced these rates of temperature change (Fig. 2b). At more moderate

rates of warming (0.5 °C/year) where data coverage was higher, 1.4% of species per year on land, 2.6% in freshwater, and 1.0% in the ocean on average were replaced (Fig. 2b). The temperature change relationships were significantly larger than expected from null distributions of model coefficients from permutation ($p = 0.001$ for terrestrial warming; $p = 0.007$ for marine warming; $p = 0.001$ for marine cooling; $p = 0.024$ for freshwater warming; and $p = 0.004$ for freshwater cooling), except for terrestrial cooling ($p = 0.067$). A downsampling sensitivity test to address non-independence of dissimilarity values within time series also supported these effects, except for the freshwater warming effect that was highly uncertain (Extended Data Fig. 4b; see Methods).

These findings are consistent with the expectations from thermal niche-based processes leading to community change, in which temperature changes alter the relative fitness and balance of interactions among species (11, 20–23). When niche-based processes are operating, both warming and cooling can drive changes in species composition, and—consistent with this prediction—we found that faster temporal turnover was associated both with higher rates of warming and with higher rates of cooling in all realms (Fig. 2b). That is, the rate of temperature change *per se* rather than its sign appears to play an important role underpinning changes in composition across taxa and realms.

We further found that the relationship between temporal turnover and temperature change differed at warmer vs. colder baseline temperatures. In terrestrial and marine assemblages, turnover responded more to warming (i.e., had higher sensitivity) at locations with warmer average temperatures, and responded more to cooling at locations with cooler average temperatures (Fig. 2c), based on a model including the interaction between temperature change, average temperature, and year (Table 1, Extended Data Fig. 5a and Table 2). This model was statistically significant ($\chi^2 = 96.2$, $df = 18$, two-sided $p = 1.1 \times 10^{-12}$, likelihood ratio test against a GLMM without this interaction), and the marine effects were also supported by a downsampling sensitivity test (Extended Data Fig. 4c). The modulating effect of average temperature in freshwater assemblages had substantial uncertainty, particularly in the downsampling test (Extended Data Fig. 4c), likely explained by the much lower availability of freshwater data. We also found that latitude was a less effective explanatory factor than average temperature (Table 1) and that alternative model formulations considering species gains and losses or focused only on longer time series produced similar results (Extended Data Table 3). Finally, when we used an abundance-based dissimilarity metric more sensitive to changes in common species, rather than the equal weighting of common and rare species in Jaccard dissimilarity (see Methods), we found similar effects of, and interactions between, temperature change and average temperatures (Extended Data Table 4; $\chi^2 = 170$, $df = 9$, two-sided $p < 2.2 \times 10^{-16}$, likelihood ratio test for the model with a temperature change effect on turnover rate against a GLMM without this effect; $\chi^2 = 377$, $df = 18$, two-sided $p < 2.2 \times 10^{-16}$, likelihood ratio test for the model with interactions between temperature change and average temperature against a GLMM without this interaction). These results suggest that the findings were not driven by simply the comings and goings of rare species, but rather by wholesale shifts in species composition through time.

There are several potential and non-mutually exclusive explanations for these results. First, many assemblages exhibit a thermal bias, such that their constituent species are on average adapted to temperatures warmer or colder than the ones they experience locally (21). Assemblages with a positive thermal bias (warm-adapted) are expected to be more sensitive to cooling, while those with a negative thermal bias (cold-adapted) are expected to be more sensitive to warming. Assemblages with positive bias are more common in colder climates, while those with a negative bias are often found in warmer climates (21, 24, 25), which predicts stronger response to cooling in cold climates and to warming in warm climates. Second, species physiological limits differ across climate gradients, such that species in cold climates live closer to their lower thermal limit, and species in warm climates live closer to their upper thermal limit (11, 26). Species in cold climates are therefore more likely to approach or exceed their limits with cooling, and those in warm climates to do so with warming. Third, assemblages may not yet have fully responded to past changes in temperature (27), which may accentuate their sensitivity to further changes in

temperature. Some evidence suggests plant assemblages in warm climates, for example, have a negative thermal bias because they have not yet responded to past warming, which therefore makes them less tolerant of further warming (27). Fourth, low niche diversity towards the ends of the global climate gradient may drive species attrition with warming in warm climates and with cooling in cold climates (28). Further research will be needed to understand the relative importance of these mechanisms and processes.

Microclimates and human transformation

One potential moderator of community responses to changing climates is whether the landscapes in which assemblages are embedded have fine-grained temperature variation that helps buffer climate change impacts (29). To test this, we measured microclimate variability as the spatial standard deviation of surface temperatures within 20 km of each site (see Methods), and found that assemblages in more homogeneous land- and seascapes were more sensitive to temperature change than in more heterogeneous ones (Fig. 3a, Extended Data Table 5; $\chi^2 = 46.8$, $df = 8$, two-sided $p = 1.7 \times 10^{-7}$, likelihood ratio test against a GLMM without microclimate terms). For example, with equally fast rates of warming, average terrestrial turnover rates in homogenous landscapes ($4.7\% \pm 0.82\%$ per year, \pm standard error) were more than twice the rates in heterogeneous landscapes ($2.3\% \pm 0.80\%$ per year, \pm standard error). The main effects of temperature change were similar in this more complex model (Extended Data Fig. 5b) to those in the simpler models reported above (Fig. 2b).

Finally, human transformation of ecosystems and climate change are two of the greatest pressures on biodiversity (3), and yet it has remained difficult to understand how their combined impacts interact (30). We found a positive interaction between non-climate human impacts like land use, pollution, and invasive species (see Methods) and temperature change on rates of temporal turnover (Fig. 3b, Extended Data Table 5; $\chi^2 = 34.1$, $df = 8$, two-sided $p = 3.8 \times 10^{-6}$, likelihood ratio test against a GLMM without human impact terms), indicating that human modifications to land- and seascapes exacerbate the impacts of temperature change. With equally fast rates of warming, terrestrial assemblages experiencing strong human impacts had more than one and a half times the turnover rates compared to those experiencing few human modifications ($4.0\% \pm 0.7\%$ per year vs. $2.1\% \pm 0.85\%$ per year, \pm standard error, Fig. 3b). The interaction between human impacts and temperature change on turnover rates on land is consistent with the hypothesis that human activity reduces microclimate availability, increases stress, alters the species pool, and/or strengthens the relative influence of abiotic factors on population dynamics (13, 30–32), all of which could increase the likelihood of resident population extirpation and of colonization by more tolerant species when temperatures change (13, 30). We detected a somewhat weaker interaction in the ocean (Fig. 3b), suggesting that harvesting—the dominant human impact affecting marine communities—has weaker or non-systematic interactions with temperature change compared to habitat degradation on land. Fishing does not substantially alter microclimate availability, for example, though habitat change in the ocean is intensifying (33).

Discussion

We found strong responses of temporal turnover to temperature change on land, in freshwater, and in the ocean. Previous research has found higher vulnerability to warming for marine species (26), and that geographic range shifts towards the poles and species richness responses to temperature change are stronger or more easily detected in the ocean than on land (13, 14). Greater thermoregulatory capacity and larger thermal safety margins on land as compared to the ocean have been suggested as reasons for limited geographic range shifts and richness changes, but substantial temporal turnover in species composition can occur without changes in richness or shifts in distributions (2). Temporal turnover therefore emerges as a particularly sensitive indicator of climate impacts in all realms.

The results further suggest that factors that could insulate ecological communities from the physiological and indirect impacts of temperature change—including behavioral adaptation and changing

biotic interactions—are insufficient in general to buffer the composition of assemblages from these environmental changes. Understanding the patterns of and processes leading to temporal turnover in the face of global change is a key issue that needs deeper investigation. Important topics include quantitative theory for temporal turnover (22, 34), understanding the role of species traits and community structure in regulating temporal turnover (22, 23), developing long time series of species composition, and addressing the taxonomic and spatial biases in existing data (35). Most of the data in the analyses come from northern temperate regions, as is typical of biodiversity data (15, 35), and the underrepresentation of high latitude regions where climate change is fastest (17) and of lower latitude regions where species vulnerability is higher (11, 26) suggest the analyses are conservative and underestimate the sensitivity of species composition to temperature change.

The impacts of climate change on individual species have often been called largely unpredictable or idiosyncratic (36). Here, we reveal that community responses may be more easily predicted: changing temperatures drive widespread turnover in species composition that scales with the speed of warming or cooling. Rates of global warming are expected to triple by the end of the century and local human impacts continue to expand (37), which will likely drive even greater rates of temporal turnover. As communities change faster, society increasingly risks ecological surprises, which may include the loss of critical ecosystem functions and services (2). Efforts to avoid further global warming, preserve microclimate variability, and reduce land use change are thus important steps towards avoiding the most undesirable of these outcomes and maintaining ecosystem integrity.

Main References and Notes

1. M. Dornelas, N. J. Gotelli, B. J. McGill, H. Shimadzu, F. Moyes, C. Sievers, A. E. Magurran, Assemblage time series reveal biodiversity change but not systematic loss. *Science* **344**, 296–9 (2014).
2. H. Hillebrand, B. Blasius, E. T. Borer, J. M. Chase, J. A. Downing, B. K. Eriksson, C. T. Filstrup, W. S. Harpole, D. Hodapp, S. Larsen, A. M. Lewandowska, E. W. Seabloom, D. B. Van de Waal, A. B. Ryabov, Biodiversity change is uncoupled from species richness trends: Consequences for conservation and monitoring. *J. Appl. Ecol.* **55**, 169–184 (2018).
3. IPBES, “Global assessment report on biodiversity and ecosystem services of the Intergovernmental Science-Policy Platform on Biodiversity and Ecosystem Services” (IPBES Secretariat, Bonn, Germany, 2019); <https://ipbes.net/global-assessment>.
4. S. A. Blowes, S. Supp, L. H. Antão, A. E. Bates, H. Bruelheide, J. M. Chase, F. Moyes, A. E. Magurran, B. J. McGill, I. H. Myers-Smith, M. Winter, A. D. Bjorkman, D. E. Bowler, J. E. K. Byrnes, A. Gonzalez, J. Hines, F. Isbell, H. P. Jones, L. M. Navarro, P. L. Thompson, M. Vellend, C. Waldock, M. Dornelas, The geography of biodiversity change in marine and terrestrial assemblages. *Science* **366**, 339–345 (2019).
5. J. M. M. Lewthwaite, D. M. Debinski, J. T. Kerr, High community turnover and dispersal limitation relative to rapid climate change. *Glob. Ecol. Biogeogr.* **26**, 459–471 (2017).
6. V. Sgardeli, K. Zografou, J. M. Halley, Climate change versus ecological drift: Assessing 13 years of turnover in a butterfly community. *Basic Appl. Ecol.* **17**, 283–290 (2016).
7. G. N. Daskalova, I. H. Myers-Smith, A. D. Bjorkman, S. A. Blowes, S. R. Supp, A. E. Magurran, M. Dornelas, Landscape-scale forest loss as a catalyst of population and biodiversity change. *Science* **368**, 1341–1347 (2020).
8. R. Nakadai, Degrees of compositional shift in tree communities vary along a gradient of temperature change rates over one decade: Application of an individual-based temporal beta-diversity concept. *Ecol. Evol.* **10**, 13613–13623 (2020).
9. M. Lindholm, J. Alahuhta, J. Heino, H. Toivonen, Temporal beta diversity of lake plants is determined by concomitant changes in environmental factors across decades. *J. Ecol.* **109**, 819–832 (2021).
10. M. J. Angilletta Jr., *Thermal Adaptation: A Theoretical and Empirical Synthesis* (Oxford University Press, Oxford, 2009).
11. J. M. Sunday, J. M. Bennett, P. Calosi, S. Clusella-Trullas, S. Gravel, A. L. Hargreaves, F. P. Leiva, W. C. E. P. Verberk, M. Á. Olalla-Tárraga, I. Morales-Castilla, Thermal tolerance patterns across latitude and elevation. *Philos. Trans. R. Soc. B Biol. Sci.* **374**, 20190036 (2019).
12. M. L. Pinsky, L. Comte, D. F. Sax, Unifying climate change biology across realms and taxa. *Trends Ecol. Evol.* **37**, 672–682 (2022).
13. J. Lenoir, R. Bertrand, L. Comte, L. Bourgeaud, T. Hattab, J. Murienne, G. Grenouillet, Species better track climate warming in the oceans than on land. *Nat. Ecol. Evol.* **4**, 1044–1059 (2020).
14. L. H. Antão, A. E. Bates, S. A. Blowes, C. Waldock, S. R. Supp, A. E. Magurran, M. Dornelas, A. M. Schipper, Temperature-related biodiversity change across temperate marine and terrestrial systems. *Nat. Ecol. Evol.* **4**, 927–933 (2020).
15. M. Dornelas, L. H. Antão, F. Moyes, A. E. Bates, A. E. Magurran, D. Adam, A. A. Akhmetzhanova, W. Appeltans, J. M. Arcos, H. Arnold, N. Ayyappan, G. Badihi, A. H. Baird, M. Barbosa, T. E. Barreto, C. Bässler, A. Bellgrove, J. Belmaker, L. Benedetti-Cecchi, B. J. Bett, A. D. Bjorkman, M. Błażewicz, S. A. Blowes, C. P. Bloch, T. C. Bonebrake, S. Boyd, M. Bradford, A. J. Brooks, J. H. Brown, H. Bruelheide, P. Budy, F. Carvalho, E. Castañeda-Moya, C. A. Chen, J. F. Chamblee, T. J. Chase, L. Siegwart Collier, S. K. Collinge, R. Condit, E. J. Cooper, J. H. C. Cornelissen, U. Cotano, S. Kyle Crow, G. Damasceno, C. H. Davies, R. A. Davis, F. P. Day, S. Degraer, T. S. Doherty, T. E. Dunn, G. Durigan, J. E. Duffy, D. Edelist, G. J. Edgar, R. Elahi, S. C. Elmendorf, A. Enemar, S. K. M. Ernest, R. Escribano, M. Estiarte, B. S. Evans, T.-Y. Fan, F. Turini Farah, L. Loureiro Fernandes, F. Z. Farneda, A. Fidelis, R. Fitt, A. M. Fosaa, G. A. Daher Correa Franco, G. E. Frank, W. R. Fraser, H. García, R. Cazzolla Gatti, O. Givan, E. Gorgone-Barbosa, W. A. Gould, C. Gries, G. D. Grossman, J. R. Gutierrez, S. Hale, M. E. Harmon, J. Harte, G. Haskins, D. L. Henshaw, L. Hermanutz, P. Hidalgo, P. Higuchi, A. Hoey, G. Van Hoey, A. Hofgaard, K. Holeck, R. D. Hollister, R. Holmes, M. Hoogenboom, C. Hsieh, S. P. Hubbell, F. Huettmann, C. L. Huffard, A. H. Hurlbert, N. Macedo Ivanauskas, D. Janík, U. Jandt, A. Jażdżewska, T. Johannessen, J. Johnstone, J. Jones, F. A. M.

- Jones, J. Kang, T. Kartawijaya, E. C. Keeley, D. A. Kelt, R. Kinnear, K. Klanderud, H. Knutsen, C. C. Koenig, A. R. Kortz, K. Král, L. A. Kuhnz, C.-Y. Kuo, D. J. Kushner, C. Laguionie-Marchais, L. T. Lancaster, C. Min Lee, J. S. Lefcheck, E. Lévesque, D. Lightfoot, F. Lloret, J. D. Lloyd, A. López-Baucells, M. Louzao, J. S. Madin, B. Magnússon, S. Malamud, I. Matthews, K. P. McFarland, B. J. McGill, D. McKnight, W. O. McLarney, J. Meador, P. L. Meserve, D. J. Metcalfe, C. F. J. Meyer, A. Michelsen, N. Milchakova, T. Moens, E. Moland, J. Moore, C. Mathias Moreira, J. Müller, G. Murphy, I. H. Myers-Smith, R. W. Myster, A. Naumov, F. Neat, J. A. Nelson, M. Paul Nelson, S. F. Newton, N. Norden, J. C. Oliver, E. M. Olsen, V. G. Onipchenko, K. Pabis, R. J. Pabst, A. Paquette, S. Pardede, D. M. Paterson, R. Pélissier, J. Peñuelas, A. Pérez-Matus, O. Pizarro, F. Pomati, E. Post, H. H. T. Prins, J. C. Priscu, P. Provoost, K. L. Prudic, E. Pulliainen, B. R. Ramesh, O. Mendivil Ramos, A. Rassweiler, J. E. Rebelo, D. C. Reed, P. B. Reich, S. M. Remillard, A. J. Richardson, J. P. Richardson, I. van Rijn, R. Rocha, V. H. Rivera-Monroy, C. Rixen, K. P. Robinson, R. Ribeiro Rodrigues, D. de Cerqueira Rossa-Feres, L. Rudstam, H. Ruhl, C. S. Ruz, E. M. Sampaio, N. Rybicki, A. Rypel, S. Sal, B. Salgado, F. A. M. Santos, A. P. Savassi-Coutinho, S. Scanga, J. Schmidt, R. Schooley, F. Setiawan, K.-T. Shao, G. R. Shaver, S. Sherman, T. W. Sherry, J. Siciński, C. Sievers, A. C. da Silva, F. Rodrigues da Silva, F. L. Silveira, J. Slingsby, T. Smart, S. J. Snell, N. A. Soudzilovskaia, G. B. G. Souza, F. Maluf Souza, V. Castro Souza, C. D. Stallings, R. Stanforth, E. H. Stanley, J. Mauro Sterza, M. Stevens, R. Stuart-Smith, Y. Rondon Suarez, S. Supp, J. Yoshio Tamashiro, S. Tarigan, G. P. Thiede, S. Thorn, A. Tolvanen, M. Teresa Zugliani Toniato, Ø. Totland, R. R. Twilley, G. Vaitkus, N. Valdivia, M. I. Vallejo, T. J. Valone, C. Van Colen, J. Vanaverbeke, F. Venturoli, H. M. Verheye, M. Vianna, R. P. Vieira, T. Vrška, C. Quang Vu, L. Van Vu, R. B. Waide, C. Waldock, D. Watts, S. Webb, T. Wesolowski, E. P. White, C. E. Widdicombe, D. Wilgers, R. Williams, S. B. Williams, M. Williamson, M. R. Willig, T. J. Willis, S. Wipf, K. D. Woods, E. J. Woehler, K. Zawada, M. L. Zettler, BioTIME: A database of biodiversity time series for the Anthropocene. *Glob. Ecol. Biogeogr.* **27**, 760–786 (2018).
16. S. L. Collins, F. Micheli, L. Hartt, A method to determine rates and patterns of variability in ecological communities. *Oikos* **91**, 285–293 (2000).
 17. E. Post, B. A. Steinman, M. E. Mann, Acceleration of phenological advance and warming with latitude over the past century. *Sci. Rep.* **8**, 3927 (2018).
 18. R. B. Millar, M. J. Anderson, N. Tolimieri, Much ado about nothings: using zero similarity points in distance-decay curves. *Ecology* **92**, 1717–1722 (2011).
 19. C. R. Muletz-Wolz, N. P. Kurata, E. A. Himschoot, E. S. Wenker, E. A. Quinn, K. Hinde, M. L. Power, R. C. Fleischer, Diversity and temporal dynamics of primate milk microbiomes. *Am. J. Primatol.* **81**, e22994 (2019).
 20. R. D. Stuart-Smith, G. J. Edgar, A. E. Bates, Thermal limits to the geographic distributions of shallow-water marine species. *Nat. Ecol. Evol.* **1**, 1–7 (2017).
 21. R. D. Stuart-Smith, G. J. Edgar, N. S. Barrett, S. J. Kininmonth, A. E. Bates, Thermal biases and vulnerability to warming in the world's marine fauna. *Nature* **528**, 88–92 (2015).
 22. J. A. Bonachela, M. T. Burrows, M. L. Pinsky, Shape of species climate response curves affects community response to climate change. *Ecol. Lett.* **24**, 708–718 (2021).
 23. I. Khaliq, C. Rixen, F. Zellweger, C. H. Graham, M. M. Gossner, I. R. McFadden, L. Antão, J. Brodersen, S. Ghosh, F. Pomati, O. Seehausen, T. Roth, T. Sattler, S. R. Supp, M. Riaz, N. E. Zimmermann, B. Matthews, A. Narwani, Warming underpins community turnover in temperate freshwater and terrestrial communities. *Nat. Commun.* **15**, 1921 (2024).
 24. R. V. Gallagher, S. Allen, I. J. Wright, Safety margins and adaptive capacity of vegetation to climate change. *Sci. Rep.* **9**, 8241 (2019).
 25. S. Peng, Y. Liu, T. Lyu, X. Zhang, Y. Li, Z. Wang, Towards an understanding of the latitudinal patterns in thermal tolerance and vulnerability of woody plants under climate warming. *Ecography* **44**, 1797–1807 (2021).
 26. M. L. Pinsky, A. M. Eikeset, D. J. McCauley, J. L. Payne, J. M. Sunday, Greater vulnerability to warming of marine versus terrestrial ectotherms. *Nature* **569**, 108–111 (2019).
 27. R. Bertrand, G. Riofrío-Dillon, J. Lenoir, J. Drapier, P. De Ruffray, J.-C. Gégout, M. Loreau, Ecological constraints increase the climatic debt in forests. *Nat. Commun.* **7**, 12643 (2016).
 28. G. Beaugrand, R. Kirby, E. Goberville, The mathematical influence on global patterns of biodiversity. *Ecol. Evol.* **10**, 6494–6511 (2020).

29. A. J. Suggitt, R. J. Wilson, N. J. B. Isaac, C. M. Beale, A. G. Auffret, T. August, J. J. Bennie, H. Q. P. Crick, S. Duffield, R. Fox, J. J. Hopkins, N. A. Macgregor, M. D. Morecroft, K. J. Walker, I. M. D. Maclean, Extinction risk from climate change is reduced by microclimatic buffering. *Nat. Clim. Change* **8**, 713 (2018).
30. J. J. Williams, T. Newbold, Local climatic changes affect biodiversity responses to land use: A review. *Divers. Distrib.* **26**, 76–92 (2020).
31. A. B. Tóth, S. K. Lyons, W. A. Barr, A. K. Behrensmeyer, J. L. Blois, R. Bobe, M. Davis, A. Du, J. T. Eronen, J. T. Faith, D. Fraser, N. J. Gotelli, G. R. Graves, A. M. Jukar, J. H. Miller, S. Pineda-Munoz, L. C. Soul, A. Villaseñor, J. Alroy, Reorganization of surviving mammal communities after the end-Pleistocene megafaunal extinction. *Science* **365**, 1305–1308 (2019).
32. A. R. Kortz, F. Moyes, V. R. Pivello, P. Pyšek, M. Dornelas, P. Visconti, A. E. Magurran, Elevated compositional change in plant assemblages linked to invasion. *Proc. R. Soc. B Biol. Sci.* **290**, 20222450 (2023).
33. D. J. McCauley, M. L. Pinsky, S. R. Palumbi, J. A. Estes, F. H. Joyce, R. R. Warner, Marine defaunation: Animal loss in the global ocean. *Science* **347**, 1255641–1255641 (2015).
34. V. J. Ontiveros, J. A. Capitán, E. O. Casamayor, D. Alonso, The characteristic time of ecological communities. *Ecology* **102**, e03247 (2021).
35. J. Hortal, F. De Bello, J. A. F. Diniz-Filho, T. M. Lewinsohn, J. M. Lobo, R. J. Ladle, Seven Shortfalls that Beset Large-Scale Knowledge of Biodiversity. *Annu. Rev. Ecol. Evol. Syst.* **46**, 523–549 (2015).
36. L. Zhang, D. Takahashi, M. Hartvig, K. H. Andersen, Food-web dynamics under climate change. *Proc. R. Soc. B Biol. Sci.* **284**, 20171772 (2017).
37. J.-Y. Lee, J. Marotzke, G. Bala, L. Cao, S. Corti, J. P. Dunne, F. Engelbrecht, E. Fischer, J. C. Fyfe, C. Jones, A. Maycock, J. Mutemi, O. Ndiaye, S. Panickal, T. Zhou, “Future Global Climate: Scenario-based Projections and Near-term Information” in *Climate Change 2021: The Physical Science Basis. Contribution of Working Group I to the Sixth Assessment Report of the Intergovernmental Panel on Climate Change*, V. Masson-Delmotte, P. Zhai, A. Pirani, S. L. Connors, C. Péan, S. Berger, N. Caud, Y. Chen, L. Goldfarb, M. I. Gomis, M. Huang, K. Leitzell, E. Lonnoy, J. B. R. Matthews, T. K. Maycock, T. Waterfield, O. Yelekçi, R. Yu, B. Zhou, Eds. (Cambridge University Press, Cambridge, UK and New York, NY, USA, 2021), pp. 553–672.

Tables

Table 1. Comparison of models of temporal turnover with or without temperature change. Lower Akaike's Information Criterion (AIC) indicates more parsimonious models (i.e., higher explanatory power without overfitting). Models with local temperature change (T_{change}) interacting with year (Year) had negative $\Delta\text{AIC}_{\text{null}}$ and were favored over the simplest Year model (dissimilarity as a function of year), while models with only realm (Realm) or only taxonomic group (Taxon) interacting with year were not favored. More complex models also included absolute latitude ($|\text{Lat}|$) or average temperature (T_{ave}) as interactions with year (see Methods for full details). Columns show degrees of freedom (df), AIC, AIC compared to the lowest AIC (ΔAIC), and AIC compared to the simplest model ($\Delta\text{AIC}_{\text{null}}$). The most parsimonious model of this set is highlighted in bold. See Extended Data Fig. 5a and Extended Data Tables 1 and 2 for additional model details. See Extended Data Table 3 for alternative model formulations.

Model	df	AIC	ΔAIC	$\Delta\text{AIC}_{\text{null}}$
Year	17	679835	746	0
Realm \times Year	19	679827	738	-8.05
Taxon \times Year	31	679846	757	10.6
($T_{\text{change}} + \text{Year}$) \times Realm	28	679794	705	-41
$T_{\text{change}} \times \text{Year} \times \text{Realm}$	37	679669	580	-166
$T_{\text{change}} \times \text{Lat} \times \text{Year} \times \text{Realm}$	61	679121	32	-714
($T_{\text{change}} + T_{\text{ave}}$) \times Year \times Realm	43	679150	60	-686
$T_{\text{change}} \times T_{\text{ave}} \times \text{Year} \times \text{Realm}$	61	679089	0	-746

Figures and Legends

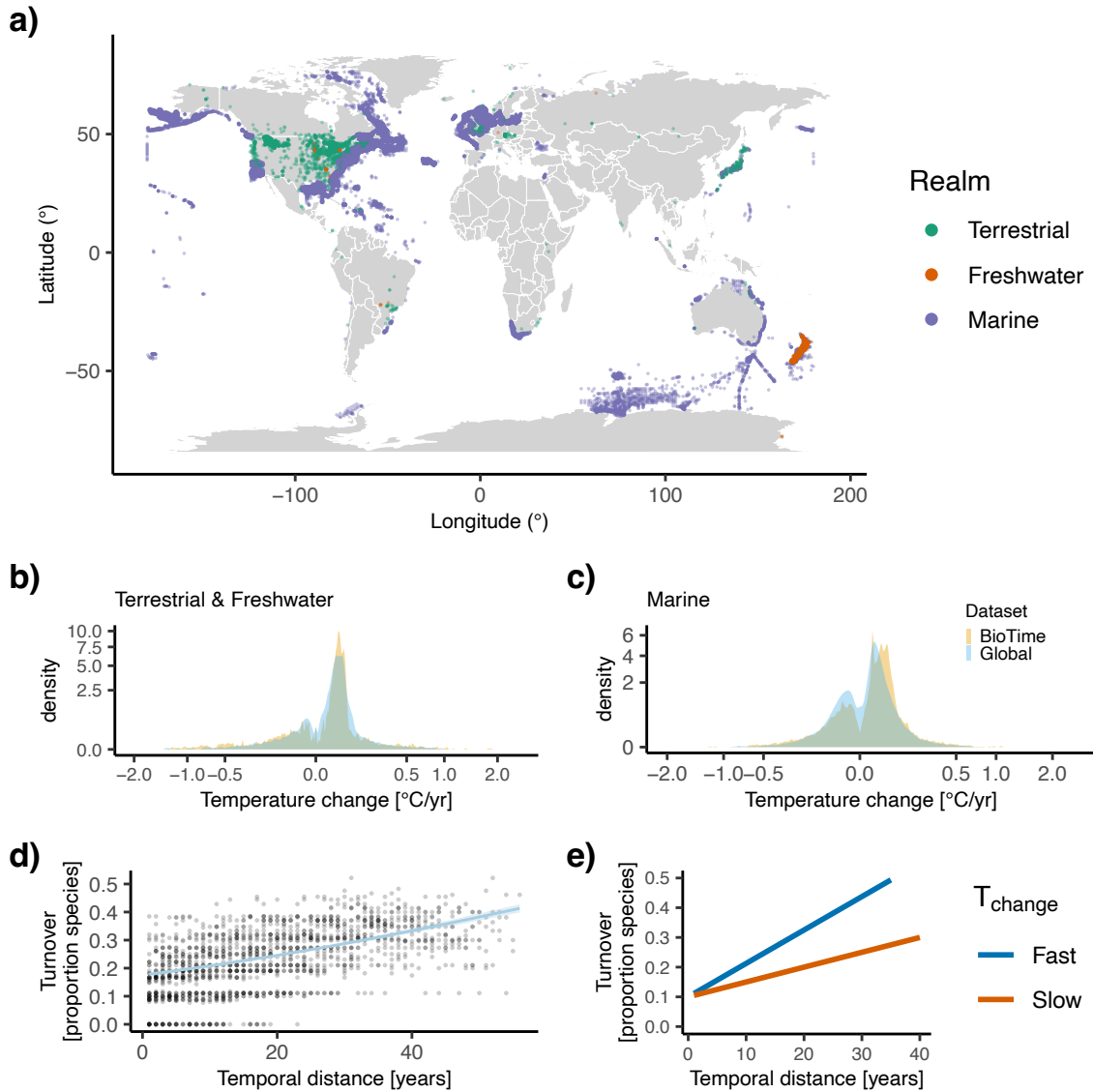
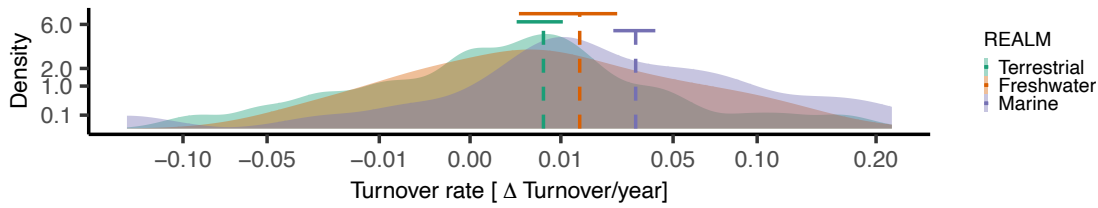
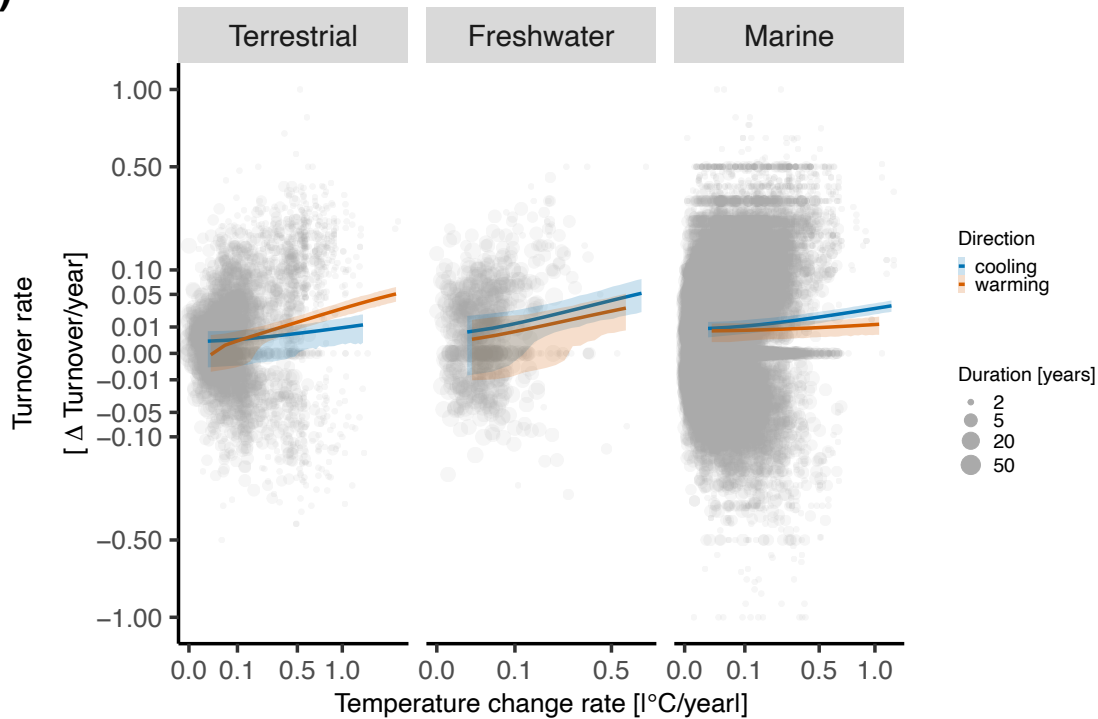


Fig. 1. Records of species composition temporal turnover from around the world. a) Location of assemblage time series from BioTIME, including 3,159 on land, 38,451 in the ocean, and 645 in freshwater. Map is from (38). b, c) Comparison of temperature change at BioTIME locations and at randomly selected sites globally with equivalent sampling intervals and durations on continents (b) or in the ocean (c). Note that the x- and y-axes have been square-root transformed to facilitate visualization. d) Example of a turnover rate calculation (ordered beta regression slope in blue), based on 57 years of bird community sampling in Sweden (39). Dissimilarity varies between 0 and 1 and was measured with the replacement component of the incidence-based Jaccard index. Slope is shown with 95% confidence intervals. e) Conceptual diagram of the statistical approach. The main hypothesis was that temporal turnover rates (slopes) differed across assemblages that experienced faster or slower rates of temperature change (T_{change}). We tested T_{change} as a continuous variable, though only two levels are shown in the diagram.

a)



b)



c)

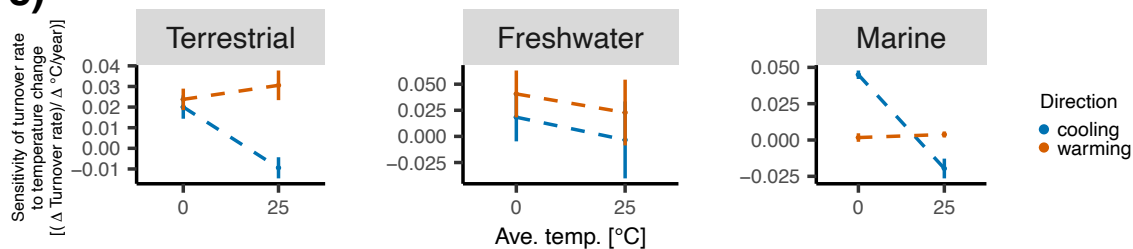


Fig. 2. Species turnover rates were related to rates of warming and cooling. a) Turnover rate [change in dissimilarity per year] for studies in terrestrial, freshwater, and marine realms. Dashed lines are the averages across studies within realms, and the top horizontal lines indicate the 95% confidence intervals for the averages. b) Marginal effects of absolute temperature change on the turnover rates with 95% confidence intervals (lines and shading) for assemblages that experienced warming or cooling (color). Translucent data points show individual time series with dot size scaled by duration. c) Marginal effects of average temperature on the turnover rate's sensitivity to temperature change for assemblages that are warming or cooling (color). Error bars show 95% confidence intervals. Similar plots with downsampling are shown in Extended Data Fig. 4b and c, which highlight the uncertainty for freshwater ecosystems. The x- and y-axes in a and b have been square-root transformed to facilitate visualization.

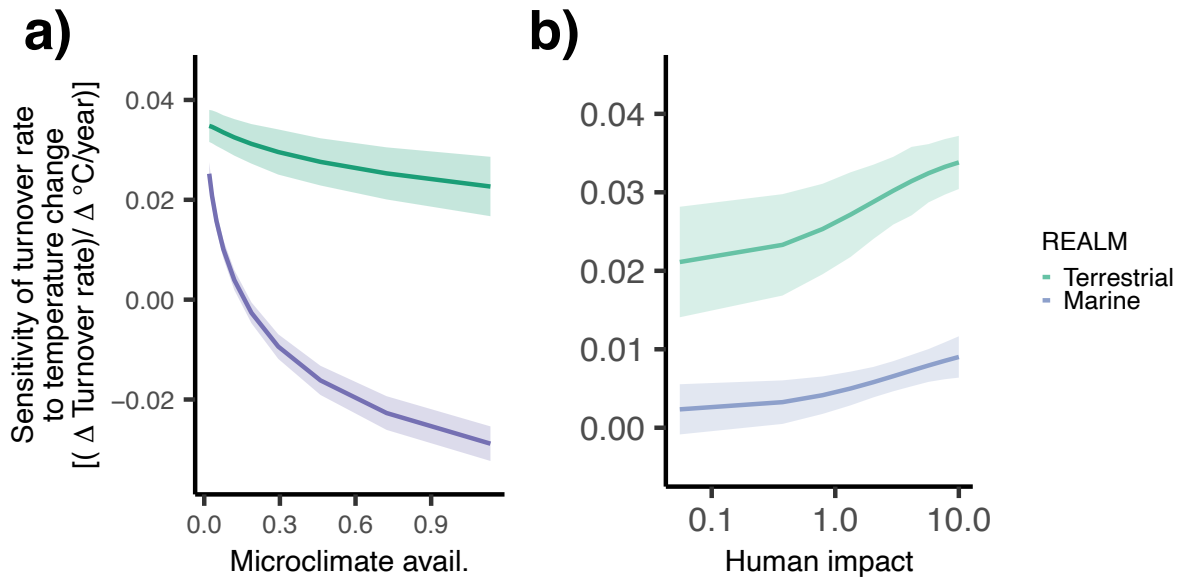


Fig. 3. Covariates associated with the sensitivity of turnover rates to temperature change in the marine and terrestrial realms. Turnover rates were more sensitive to changing temperatures when a) environments had less microclimate availability (measured as the standard deviation of temperature within a 20 km radius, °C), or b) human impacts were greater, particularly on land (low-to-high index from 0 to 10). The heavy line is the mean and the shaded area represents the 95% confidence interval.

Methods

Data description

We examined biodiversity change using the BioTIME database, which is the largest global compilation of species assemblage time series (15). We used time series of species composition or abundance from 319 individual studies. Because we were interested in analyzing local biodiversity change, we followed Blowes et al. (4) and gridded studies with multiple sampling locations and extents greater than 71.7 km² ($n = 147$ studies) into 96 km² equal area icosahedral hexagonal grid cells (40). This threshold has been previously identified as the mean plus one standard deviation of the spatial extent in single-location studies (4). We assigned studies with a single location and those with extents < 71.7 km² to the grid cell in which their center latitude and longitude were located. The sample locations from all other studies were assigned to cells based on the latitude and longitude of individual samples. We then collated species within each unique study-cell combination for each year (i.e., samples from different studies were not combined when they were in the same cell), resulting in assemblage time series within grid cells. This approach allowed us to assess the effects of the different environmental drivers at a standardized resolution between studies and across realms.

To minimize sampling effects in our estimates, we first calculated the abundance-based coverage (41) of each (annual) sample within each cell-level time series. We then removed all samples with coverage less than 0.85. This threshold meant that there was a <15% chance that another sample in any given year of one more individual would represent a new species. We also removed time series with fewer than five unique taxa or with less than ten individuals. In total, this process yielded 42,255 time series distributed among 41,483 locations. Most time series were started in the second half of the 20th century and were less than 40 years long, with a median length of 8 years (Extended Data Fig. 1).

Our final dataset included 3,159 terrestrial; 38,451 marine; and 645 freshwater time series across a wide range of taxa, including birds (8,356 time series), mammals (259), fishes (24,334), amphibians and reptiles (339), invertebrates (2,577), and plants (285). Individual time series in this database generally focused on a single guild of organisms (e.g., birds or fishes). The time series were located across nearly the full range of latitudes and longitudes (Fig. 1a), and spanned effectively the full range of changes in surface temperatures observed globally (Fig. 1b,c). However, the time series were more densely concentrated in the Northern hemisphere and at temperate latitudes (Fig. 1a).

We calculated dissimilarity between each pair of annual samples within each time series (2). We did not include any years compared to themselves (i.e., zero dissimilarity at zero difference in time) because doing so introduces a positive bias in temporal turnover rates, particularly for shorter time series. Before calculating dissimilarity, we used sample-based rarefaction to standardize the number of samples per year within each time series. This procedure helped prevent temporal variation in sampling effort from affecting diversity estimates (42). First, we identified the minimum number of samples taken in a year within each time series. This minimum was then used to randomly resample each year down to that number of samples. We then calculated pairwise Jaccard dissimilarity between each pair of years. We repeated this process 199 times for each time series and took the median dissimilarities. We partitioned total Jaccard dissimilarity into the components of species replacement and changes in the number of species (43, 44). Because the replacement component dominates biodiversity change (4), we focused our analysis here on replacement, i.e. the component quantifying species replacement independent of changes in species richness.

In addition, we calculated pairwise Morisita-Horn dissimilarity, which also accounts for changes in species abundance and, in particular, is sensitive to changes in the more abundant species, making it less vulnerable to under-sampling (45, 46). We then proceeded with the analysis below (see *Statistical models with and without temperature*), using Morisita-Horn dissimilarity in place of the replacement component of Jaccard dissimilarity.

Statistical models with and without temperature

The rate of change in species composition (temporal turnover rate) is typically measured as the slope of dissimilarity vs. time (1, 4, 16). Steeper slopes indicate faster rates of biodiversity change through time. However, analysis of these data across many time series poses certain statistical challenges. First, dissimilarity is constrained from 0 and 1 but does not have a straightforward measure of sample size as, for example, binomial samples do. Continued turnover in species composition for two assemblages leads to dissimilarity that asymptotes at one. In addition, the dataset has multiple measures of dissimilarity from each time series and multiple time series from some studies, creating pseudoreplication. The time series also differ in duration, which affects the variance of their slopes and introduces strong heteroskedasticity (Extended Data Fig. 2).

After testing a set of potential approaches (see *Comparison of alternative statistical approaches*), we chose a generalized linear mixed model (GLMM) with ordered beta errors (47) and a logit link function in which dissimilarity ($D_{i,j,s,t}$) between each pair of annual samples in time series j from study i between years s and t was modeled as a function of the number of years elapsed between those samples ($Years_{s,t}$). The logit link helped to account for the non-linear response of dissimilarity to ongoing composition change such that dissimilarity could asymptote at one as elapsed years increased towards infinity, while the ordered beta errors helped account for the fact that observations were constrained between and including 0 and 1. To address pseudoreplication, we included random intercepts ($\beta_{0,i}; \beta_{0,i,j}$) and random slopes for $Years$ ($\beta_{1,i}; \beta_{1,i,j}$) for each time series j nested within each study i in all models. The intercept represented the predicted dissimilarity of independent samples taken at the same time (zero time elapsed), and so captured factors including but not limited to differences in species pool size, sample size, sampling effort, sample completeness, and measurement error. We included an interaction between initial dissimilarity and elapsed years ($D_{i,j,init}: Years_{s,t}$) to account for the fact that initial dissimilarity can influence the rate of temporal turnover (48). Initial dissimilarity was the average dissimilarity at the minimum elapsed years between samples in a time series. Based on visual inspection of the residuals, we also allowed the intercept and precision (ϕ , inverse of dispersion) to differ between realms (terrestrial, marine, and freshwater). The baseline model (the “Year” model) was therefore defined by

$$D_{i,j,s,t} \sim \text{OrdBeta}(\mu_{i,j,s,t}, \phi_0 + \phi_1 \text{Realm}_{i,j}^{\text{Marine}} + \phi_2 \text{Realm}_{i,j}^{\text{Terrestrial}}) \quad \text{Eq. 1}$$

and

$$\text{logit}(\mu_{i,j,s,t}) \sim \alpha_0 + \alpha_1 \text{Realm}_{i,j}^{\text{Marine}} + \alpha_2 \text{Realm}_{i,j}^{\text{Terrestrial}} + \alpha_3 \text{Years}_{s,t} + \alpha_4 D_{i,j,init} + \alpha_5 D_{i,j,init} \text{Years}_{s,t} + \beta_{0,i} + \beta_{0,i,j} + (\beta_{1,i} + \beta_{1,i,j}) \text{Years}_{s,t}$$

with fixed effects α , random effects for intercept and slope by study ($(\beta_{0,i}; \beta_{1,i}) \sim \text{MVN}(0, \Sigma_{\text{study}})$) and by time series ($(\beta_{0,i,j}; \beta_{1,i,j}) \sim \text{MVN}(0, \Sigma_{\text{timeseries}})$), and indicator variables (1 if true, 0 if false) for whether each time series was marine or terrestrial instead of freshwater ($\text{Realm}_{i,j}^{\text{Marine}}$ and $\text{Realm}_{i,j}^{\text{Terrestrial}}$). The α_1 and α_2 terms indicated the difference between the baseline (freshwater) and either marine or terrestrial realms, respectively.

We then implemented more complex models to test specific hypotheses (Table 1). The first more complex model (the “Realm \times Year” model) tested for different rates of temporal turnover among realms by including an interaction between realm and the number of years elapsed between samples (i.e., $\text{Realm}:\text{Years}$). A larger coefficient for a given realm would indicate a faster rate of turnover compared to other realms. We also fit a taxonomic model (the “Taxon \times Year” model) that used taxonomic groups in place of realm. We used the groupings identified in the BioTIME dataset: plants, fishes, invertebrates,

birds, benthos (renamed as “benthic species” to facilitate interpretation), mammals, amphibians, reptiles, and multiple taxa (the latter indicating studies that examined more than one group).

The next model (the “ $T_{\text{change}} \times \text{Year} \times \text{Realm}$ ” model) tested our core hypothesis that the rate of temporal turnover differed for assemblages that had experienced different rates of temperature change, and whether this relationship differed between realms. To do this, we extracted all mean annual temperatures between and including the start and end years of each biodiversity time series at the corresponding latitude and longitude of each biodiversity time series from the CRU TS 4.03 (0.5 x 0.5° resolution) data on land and from the ERSST v5 (2 x 2° resolution, surface temperature) dataset in the ocean (49, 50). We calculated the average rate of temperature change for each biodiversity time series as the slope of temperature vs. year. We used the Theil-Sen slope, which is a standard non-parametric method with low sensitivity to outliers or start year effects (51, 52). To reflect the hypothesis that the rate of temporal turnover was associated with the rate of temperature change, the statistical model included an interaction between the magnitude (absolute value) of the temperature change rate (T_{change} , measured in degrees Celsius per year), and the elapsed number of years between samples. A positive interaction coefficient would indicate faster rates of turnover with faster temperature change. We included the sign of temperature change (*sign*) so that responses to warming and cooling would be estimated separately. If we had instead used the raw rate of temperature change (negative for cooling, positive for warming), strong cooling responses would have counterintuitively been constrained to be the opposite of strong warming responses, with intermediate responses to no temperature change. We estimated the T_{change} relationship independently for each realm because evidence suggests that rates of range shift and species additions and losses in response to temperature change differ among realms (12–14). Our full $T_{\text{change}} \times \text{Year} \times \text{Realm}$ model was therefore the baseline Year model (Eq. 1) with added terms for $\text{sign} \times T_{\text{change}} \times \text{Years} \times \text{Realm}$, in which *sign* and *Realm* were factors with two and three levels, respectively. We centered T_{change} and standardized it to a variance of one to facilitate model fitting. Our null hypothesis in this case was that dissimilarity was associated with elapsed number of years, realm, initial dissimilarity, and time series identity (see previous paragraphs for model structure descriptions), but that turnover rate was not consistently associated with the rate of temperature change. We tested the hypothesis by comparing the $T_{\text{change}} \times \text{Year} \times \text{Realm}$ model to a model with the interactions between temperature change and *Years* removed. We called the latter the $(T_{\text{change}} + \text{Year}) \times \text{Realm}$ model.

The fact that lifespans, thermal niche breadths, and biological rates differ consistently across temperature gradients suggests that the temperature change response may depend on the average temperature (11, 20, 53–55). To address this, we included an interaction between temperature change and average temperature (the “ $T_{\text{change}} \times T_{\text{ave}} \times \text{Year} \times \text{Realm}$ ” model). We measured average temperature (T_{ave} , measured in degrees Celsius) as the average across all years between and including the first and last years in each biodiversity time series. Annual temperatures were obtained as described in the previous paragraph. The $T_{\text{change}} \times T_{\text{ave}} \times \text{Year} \times \text{Realm}$ model was therefore the $T_{\text{change}} \times \text{Year} \times \text{Realm}$ model (previous paragraph) with added terms for $\text{sign} \times T_{\text{change}} \times T_{\text{ave}} \times \text{Years} \times \text{Realm}$. We centered T_{ave} and standardized it to a variance of one to facilitate model fitting. We tested the influence of T_{ave} on the

T_{change} response by comparing the $T_{\text{change}} \times T_{\text{ave}} \times \text{Year} \times \text{Realm}$ model to a model with the interactions between T_{change} and T_{ave} removed. We called the latter the $(T_{\text{change}} + T_{\text{ave}}) \times \text{Year} \times \text{Realm}$ model.

We also fit a model in which we used the absolute value of latitude in place of average temperature, to test whether distance from the equator was a simpler explanation than average temperature. Additionally, we simulated turnover in communities with higher or lower species richness to test whether higher richness at higher temperatures could explain a T_{ave} effect; we found that it did not.

Sample sizes for Jaccard dissimilarity models were 1,134,799 pairwise dissimilarities from 40,332 time series in 304 studies that had temperature and environmental covariate data available. Slightly fewer Morisita-Horn dissimilarities were available because time series had to report abundance, not just species occurrence (1,104,567 dissimilarities from 39,227 time series in 264 studies). We fit models in the *glmmTMB* package v. 1.1.8 (56) in R version 4.3.2 (57) and evaluated model assumptions with the *DHARMA* package v. 0.4.6 (58).

To display model predictions, we plotted estimates of temporal turnover rates (change in dissimilarity/year) or estimates of sensitivity to temperature change (change in turnover rate per change in rate of temperature change) instead of the pairwise dissimilarities between years, since turnover rate and sensitivity were the measures of interest. To carry the uncertainty in model predictions through to uncertainty in the predicted slopes of dissimilarity vs. year, we sampled from the uncertainty in each point prediction of dissimilarity using Gaussian distributions, fit linear estimates of temporal turnover, and repeated the process 1000 times to generate a mean and standard error of turnover rates. We repeated the process to calculate uncertainty of sensitivity. We report 95% confidence intervals as 1.96 times the standard deviations across resampling trials for both metrics. To calculate the maximum turnover rate, we trimmed the $T_{\text{change}} \times \text{Year} \times \text{Realm}$ model predictions of turnover rate to the range of observed temperature change rates within each realm and identified the maximum rate in any realm.

We compared models with Akaike's Information Criterion (AIC), which assigns lower AIC to more parsimonious models (i.e., higher explanatory power without over-fitting) (59). We also conducted two-sided likelihood ratio tests of nested models to further gauge support for specific hypotheses. Given the complexity of our dataset, we also used reshuffling to test the statistical significance of the effect of T_{change} on turnover rate by reshuffling T_{change} across time series and refitting the $T_{\text{change}} \times \text{Year} \times \text{Realm}$ model.

We repeated this process 1000 times to create a null distribution of *sign*: T_{change} :*Realm*:*Years* coefficients in which T_{change} was not associated with turnover rates. We then compared the six observed coefficients (one each for terrestrial, marine, and freshwater warming and cooling) against the corresponding null distribution and calculated a reshuffling p-value as $(x+1)/(n+1)$, where x was the number of reshuffles with a coefficient greater or equal to the observed value, and n was the number of reshuffles (60).

To more fully examine uncertainty, we also downsampled the dissimilarities within each time series. Time series of length y contained $y(y-1)/2$ pairwise dissimilarities, which were not all independent because multiple dissimilarities relied on the same observation of species composition. We therefore downsampled the dissimilarity time series to y dissimilarities, refit the $T_{\text{change}} \times \text{Year} \times \text{Realm}$ model, extracted the six marginal effects of T_{change} (for each of terrestrial, marine, and freshwater warming and cooling), and repeated the process 1000 times. We also refit the $T_{\text{change}} \times T_{\text{ave}} \times \text{Year} \times \text{Realm}$ model, extracted the sensitivity to temperature change across T_{ave} levels, and repeated the process 1000 times.

Theory suggests that the rate of dissimilarity can depend on whether species are being gained or lost and that the magnitude of this effect depends on the initial dissimilarity between assemblages (48). To test whether this process might affect our results, we calculated the relative proportion of species gains

and losses ($propGL$) in each pairwise dissimilarity as the \log_{10} ratio of the number of gains divided by the number of losses. We added one to the numerator and denominator to avoid infinite values. Data were available for 1,104,567 dissimilarities in 39,277 time series in 264 studies. We then refit our models while including a term for the interaction of initial dissimilarity, gains and losses, and the duration between observations ($D_{init}:propGL:Years$). We included a random effect only for study because models that additionally had a random effect for time series nested within study had difficulty converging. The results (Extended Data Table 3) similarly supported a relationship of turnover rate to the rate of temperature change, and also supported an interaction between average temperature and the rate of temperature change. As another sensitivity analysis, we explored fitting the models to only time series ≥ 7 years in duration and found equivalent results to those reported in the main manuscript (Extended Data Table 3).

Statistical models with environmental covariates

Theory and empirical patterns suggest that the impacts of temperature change on biodiversity change depend on the environmental context (13, 61–63). We therefore tested whether environmental covariates modified the effects of temperature change by adding the interaction between the covariate (cov) and the temperature change effect. The covariate model was therefore the $T_{change} \times T_{ave} \times Year \times Realm$ model with added terms $cov \times T_{change} \times Realm \times Years$. As covariates, we tested microclimate variability and human impact based on hypotheses for their strong importance for biodiversity change (13, 61). We measured microclimate variability as the spatial standard deviation of time-averaged surface temperature across all grid cells within 20 km of the central latitude and longitude of each assemblage time series. We used temperature data from Worldclim 2.0 on land (30 arcsec resolution, ~ 1 km) and Bio-ORACLE 2.2 in the ocean (5 arcmin resolution, ~ 9 km) (64, 65) to calculate microclimate variability. Our index of human impact was the Bowler *et al.* (66) aggregate across measures of land conversion, fishing activities, human population density, pollution, and potential for alien species invasion, thereby capturing the multiplicity of avenues by which humans modify the landscape and seascape. We excluded climate change indices from our metric of human impact to avoid double-counting. We standardized each covariate to a mean of zero and variance of one to facilitate model fitting. For AIC and likelihood ratio tests, we compared the covariate models against the Year model and against the $T_{change} \times T_{ave} \times Year \times Realm$ model. We fit models to the 39,689 time series in terrestrial and marine realms and excluded freshwater given the much smaller dataset available for this latter realm.

Comparison of alternative statistical approaches

The slopes of species compositional dissimilarity and temperature time series both contained strong heteroskedasticity because longer-duration time series had smaller variances (Extended Data Fig. 2b, c). The magnitudes of temporal turnover also declined with time series duration (Extended Data Fig. 2b). This heteroskedasticity is a general characteristic when combining time series of different durations, and these patterns also appeared in time series composed of Gaussian white noise (Extended Data Fig. 2d). Since heteroskedasticity can violate statistical testing assumptions and inflate false positive rates, we tested different statistical approaches using simulated datasets to identify methods with acceptably low false positive rates.

The test was constructed by simulating datasets analogous to time series of species dissimilarities at increasing temporal distances, which were paired with time series of an environmental covariate like temperature. The first time series of each pair consisted of dissimilarities that increased with temporal

distance and explicitly included pseudoreplication and non-linearity of species composition turnover (i.e., to mimic the downsampled species dissimilarities from empirical time series). The second time series represented an uncorrelated environmental explanatory variable (such as temperature) and was defined by Gaussian white noise with mean of 0 and standard deviation of 1. This second time series had the same duration as the dissimilarity time series. For each dataset, we simulated 1000 pairs of time series—which we pooled into 50 studies with 20 time series pairs each—to capture the hierarchical nature of our empirical dataset (i.e. pseudoreplication within studies and within time series).

Each element of the first time series in each pair (i.e. the response variable) was generated following:

$$\text{logit}(y_{ijt}) = D.\text{init}_{ij} + (\beta_i + \beta_{ij} - 0.01 \times D.\text{init}_{ij}) \times t + \varepsilon_{ijt} \quad \text{Eq. 2}$$

where y_{ijt} represents species composition dissimilarity in time series j from study i at time t ; $D.\text{init}_{ij}$ represents the initial dissimilarity and is therefore the intercept, uniformly sampled for each time series between 0 and 0.8; β_i is the slope associated with study i , uniformly distributed between 0 and 0.03; β_{ij} is the time series-specific slope uniformly distributed between 0 and 0.005; and ε_{ijt} represents a Gaussian white noise of mean 0 and standard deviation 0.1. The equation also included a term reducing the dissimilarity slope with time by a small fraction of the value of the original dissimilarity ($D.\text{init}_{ij}$) to represent the potential influence of this original dissimilarity on the rate of change (48). We used the inverse-logit transformation to constrain the simulated dissimilarity values to the interval [0, 1] and to introduce non-linearity.

In addition, we evaluated the effects of time series duration in our simulated datasets. Specifically, the simulated datasets differed in whether all the time series pairs were of the same duration (and therefore did not suffer from heteroskedasticity) or whether the durations differed among pairs, as in many ecological syntheses of biodiversity change. For the equal-duration datasets, we generated time series that were all 10 years long. For the variable-duration datasets, we generated a variety of small and large ranges of durations by generating time series between 3 and 12 (small range), 3 and 27, 3 and 52, or 3 and 102 years (large range). Durations of individual pairs of time series within a dataset were evenly distributed between the minimum and maximum.

We then fit a series of statistical models to each dataset to test for an association between the slopes of the time series in each pair under a null model of no correlation. This approach was analogous to testing for a correlation between temporal turnover rates (response) and the rate of temperature change (explanatory variable). The first statistical model tested for a non-zero Pearson product moment correlation between the slopes of the response and explanatory variables. We calculated the slope of each time series with a linear regression. We then used the absolute value of the explanatory time series slope to represent the magnitude of a temperature change.

The second statistical approach was a meta-analytical model that weighted the response values by their uncertainty, similar to those used in previous ecological time series syntheses (14). The statistical model fitted the slope of the dissimilarity time series (estimated previously using a linear regression) as a function of the slope of the explanatory variable (also estimated previously using a linear regression) in glmmTMB (56) with a random intercept by study. To downweight more uncertain slopes, we specified that dispersion in the mixed effects model was related to the standard error of the response variable slope.

The third approach was a one-stage mixed model fit directly to the response variable values, rather than to slopes of the response variable time series. We tested the hypothesis that time series with stronger trends in the explanatory variable had faster rates of change in dissimilarity (i.e., more positive slopes). The model therefore included time, the absolute value of the explanatory variable slope, and an interaction between the explanatory variable slope and time. We tested the hypothesis by examining whether the

interaction between the explanatory variable slope and time was statistically significant. To account for initial dissimilarity, we also included terms for initial dissimilarity and its interaction with time. Because each time series had multiple response values and time series were nested within studies, we also included random intercepts and slopes for time series nested within studies to account for this pseudoreplication. The model was fit in glmmTMB with Gaussian errors. These errors may not be appropriate because the response time series was constrained to the interval [0, 1].

Finally, we fit a one-stage generalized linear mixed model with ordered beta errors in glmmTMB (i.e., a GLMM). The fixed and random effects were the same as the previous approach, and the beta error with logit link term accounted for the fact that the response time series was constrained to [0, 1].

We simulated 600 datasets (each with 1000 pairs of time series) for each kind of duration range to examine false-positive rates. A false positive was counted if a given statistical test on a given dataset reported $p < 0.05$. Since the time series pairs were simulated to be uncorrelated, we would expect 5% of the datasets to produce $p < 0.05$ under the null hypothesis that we simulated. Values substantially higher than this would be of concern.

All methods had low false positive rates when datasets were composed of time series of all the same length (Extended Data Fig. 2e). The only method that retained low false positive rates with datasets composed of different-length time series was the GLMM with beta errors (Extended Data Fig. 2e). We used this latter method for all analyses.

Data availability

Species composition data are available from BioTIME (<https://biotime.st-andrews.ac.uk/>), human impact data from Bowler et al. 2020 (pan310071-sup-0003-Supinfo2.7z from <https://doi.org/10.1002/pan3.10071>), sea surface temperature from ERSST v5 (<ftp://ftp.cdc.noaa.gov/Datasets/noaa.ersst.v5/sst.mnmean.nc>), land surface temperature from CRU TS v.4.03 (http://data.ceda.ac.uk/badc/cru/data/cru_ts/cru_ts_4.03/data/cru_ts4.03.1901.2018.tmp.dat.nc), terrestrial microclimate data from WorldClim 2.0 (wc2.0_bio_30s_01.tif from <https://worldclim.org>), and marine microclimate data from Bio-ORACLE 2.2 (<https://www.bio-oracle.org/>). Please see <https://doi.org/10.5281/zenodo.13905417> for additional details.

Code availability

Scripts are available from <https://doi.org/10.5281/zenodo.13905417>.

Methods References

38. R. A. Becker, A. R. Wilks, R. Brownrigg, T. P. Minka, A. Deckmyn, maps: Draw Geographical Maps. R package, version 3.4.1 (2022); <https://CRAN.R-project.org/package=maps>.
39. S. Svensson, A. M. Thorner, N. E. I. Nyholm, Species trends, turnover and composition of a woodland bird community in southern Sweden during a period of fifty-seven years. *Ornis Svec.* **20** (2010).
40. R. Barnes, K. Sahr, dggridR: Discrete Global Grids for R. R package version 2.0.4. <https://github.com/r-barnes/dggridR/>, (2017); <https://doi.org/10.5281/zenodo.1322866>.
41. A. Chao, L. Jost, Coverage-based rarefaction and extrapolation: standardizing samples by completeness rather than size. *Ecology* **93**, 2533–2547 (2012).
42. N. J. Gotelli, R. K. Colwell, “Estimating species richness” in *Biological Diversity: Frontiers in Measurement and Assessment*, A. E. Magurran, B. J. McGill, Eds. (Oxford University Press, Oxford, UK, 2011), pp. 39–54.
43. A. Baselga, Partitioning the turnover and nestedness components of beta diversity: Partitioning beta diversity. *Glob. Ecol. Biogeogr.* **19**, 134–143 (2010).
44. A. Baselga, D. Orme, S. Villeger, J. De Bortoli, F. Leprier, M. Logez, R. Henriques-Silva, Package “betapart” version 1.5.2: Partitioning Beta Diversity into Turnover and Nestedness Components, (2020); <https://CRAN.R-project.org/package=betapart>.
45. A. E. Magurran, *Ecological Diversity and Its Measurement* (Croom Helm, London, 1988).
46. A. Chao, L. Jost, S. C. Chiang, Y.-H. Jiang, R. L. Chazdon, A Two-Stage Probabilistic Approach to Multiple-Community Similarity Indices. *Biometrics* **64**, 1178–1186 (2008).
47. R. Kubinec, Ordered Beta Regression: A Parsimonious, Well-Fitting Model for Continuous Data with Lower and Upper Bounds. *Polit. Anal.* **31**, 519–536 (2023).
48. K. C. Rosenblad, D. F. Sax, A new framework for investigating biotic homogenization and exploring future trajectories: oceanic island plant and bird assemblages as a case study. *Ecography* **40**, 1040–1049 (2017).
49. I. Harris, T. J. Osborn, P. Jones, D. Lister, Version 4 of the CRU TS monthly high-resolution gridded multivariate climate dataset. *Sci. Data* **7**, 109 (2020).
50. B. Huang, P. W. Thorne, V. F. Banzon, T. Boyer, G. Chepurin, J. H. Lawrimore, M. J. Menne, T. M. Smith, R. S. Vose, H.-M. Zhang, Extended Reconstructed Sea Surface Temperature, Version 5 (ERSSTv5): Upgrades, Validations, and Intercomparisons. *J. Clim.* **30**, 8179–8205 (2017).
51. H. Theil, A rank-invariant method of linear and polynomial regression analysis. I, II, III. *Proc. Akadademie Van Wet. Amst.* **53**, 386–392 (1950).
52. P. K. Sen, Estimates of the Regression Coefficient Based on Kendall’s Tau. *J. Am. Stat. Assoc.* **63**, 1379–1389 (1968).
53. S. B. Munch, S. Salinas, Latitudinal variation in lifespan within species is explained by the metabolic theory of ecology. *Proc. Natl. Acad. Sci. U. S. A.* **106**, 13860–4 (2009).
54. M. E. Dillon, G. Wang, R. B. Huey, Global metabolic impacts of recent climate warming. *Nature* **467**, 704–6 (2010).
55. J. H. Brown, J. F. Gillooly, A. P. Allen, V. M. Savage, G. B. West, Toward a metabolic theory of ecology. *Ecology* **85**, 1771–1789 (2004).
56. M. Brooks E., K. Kristensen, K. Benthem J., van, A. Magnusson, C. Berg W., A. Nielsen, H. Skaug J., M. Mächler, B. Bolker M., glmmTMB Balances Speed and Flexibility Among Packages for Zero-inflated Generalized Linear Mixed Modeling. *R J.* **9**, 378 (2017).
57. R Core Team, R: A Language and Environment for Statistical Computing. <https://www.R-project.org/>, R Foundation for Statistical Computing (2023).
58. F. Hartig, “DHARMA: Residual Diagnostics for Hierarchical (Multi-Level/Mixed) Regression Models. R package version 0.4.0.,” <https://CRAN.R-project.org/package=DHARMA>.
59. K. P. Burnham, D. R. Anderson, *Model Selection and Multimodel Inference: A Practical Information-Theoretic Approach* (Springer New York, New York, NY, 2002; <http://link.springer.com/10.1007/b97636>).
60. B. V. North, D. Curtis, P. C. Sham, A note on the calculation of empirical P values from Monte Carlo procedures. *Am. J. Hum. Genet.* **71**, 439–441 (2002).
61. F. Zellweger, P. De Frenne, J. Lenoir, P. Vangansbeke, K. Verheyen, M. Bernhardt-Römermann, L. Baeten, R. Hédli, I. Berki, J. Brunet, H. Van Calster, M. Chudomelová, G. Decocq, T.

- Dirnböck, T. Durak, T. Heinken, B. Jaroszewicz, M. Kopecký, F. Máliš, M. Macek, M. Malicki, T. Naaf, T. A. Nagel, A. Ortmann-Ajkai, P. Petřík, R. Pielech, K. Reczyńska, W. Schmidt, T. Standovár, K. Świerkosz, B. Teleki, O. Vild, M. Wulf, D. Coomes, Forest microclimate dynamics drive plant responses to warming. *Science* **368**, 772–775 (2020).
62. K. J. Kroeker, L. E. Bell, E. M. Donham, U. Hoshijima, S. Lummis, J. A. Toy, E. Willis-Norton, Ecological change in dynamic environments: Accounting for temporal environmental variability in studies of ocean change biology. *Glob. Change Biol.* **26**, 54–67 (2020).
63. M. K. Thomas, M. Aranguren-Gassis, C. T. Kremer, M. R. Gould, K. Anderson, C. A. Klausmeier, E. Litchman, Temperature–nutrient interactions exacerbate sensitivity to warming in phytoplankton. *Glob. Change Biol.* **23**, 3269–3280 (2017).
64. S. E. Fick, R. J. Hijmans, Worldclim 2: New 1-km spatial resolution climate surfaces for global land areas. *Int. J. Climatol.* **37**, 4302–4315 (2017).
65. J. Assis, L. Tyberghein, S. Bosch, H. Verbruggen, E. A. Serrão, O. De Clerck, D. Tittensor, Bio-ORACLE v2.0: Extending marine data layers for bioclimatic modelling. *Glob. Ecol. Biogeogr.* **27**, 277–284 (2018).
66. D. E. Bowler, A. D. Bjorkman, M. Dornelas, I. H. Myers-Smith, L. M. Navarro, A. Niamir, S. R. Supp, C. Waldock, M. Winter, M. Vellend, S. A. Blowes, K. Böhning-Gaese, H. Bruelheide, R. Elahi, L. H. Antão, J. Hines, F. Isbell, H. P. Jones, A. E. Magurran, J. S. Cabral, A. E. Bates, Mapping human pressures on biodiversity across the planet uncovers anthropogenic threat complexes. *People Nat.* **2**, 380–394 (2020).

Acknowledgments:

We thank K. Lew and J. Hauser for help with data entry; M. Stein for statistical advice; A. Bates, C. Meyer, R. Remelgado, and the Global Change Research Group at Rutgers University and the University of California Santa Cruz for useful discussions; Z. Kitchel, A. Maureaud, and P. Morin for feedback on earlier drafts; the BioTIME consortium for their commitment to open science; and the Rutgers School of Environmental and Biological Sciences for access to the Annotate and Annotate2 scientific workstations. Views and opinions expressed are those of the author(s) only and do not necessarily reflect those of the European Union or the European Research Council. Neither the European Union nor the granting authority can be held responsible for them.

Funding:

German Centre for Integrative Biodiversity Research (iDiv) Halle-Jena-Leipzig, funded by the German Research Foundation #FZT 118 and by the European Union (MLP, SAB, JMC)
Helmholtz Institute for Functional Marine Biodiversity (MLP, HH)
U.S. National Science Foundation #DEB-1616821 (MLP)
U.S. National Science Foundation #CBET-2137701 (MLP)
U.S. National Science Foundation #DEB-2129351 (MLP)
Academy of Finland grant 340280 (LHA)

Authors contributions:

Conceptualization: MLP
Data curation: SAB, MLP, BG, LHA, MTB, MRH
Formal Analysis: MLP
Funding acquisition: MLP, HH, JMC, UB
Methodology: MLP, SAB, JMC, MTB, HH, BR
Project administration: MLP
Software: MLP, SAB, LHA
Visualization: MLP
Writing – original draft: MLP, HH
Writing – review & editing: MLP, LHA, JMC, BG, SAB, UB, MRH, BR

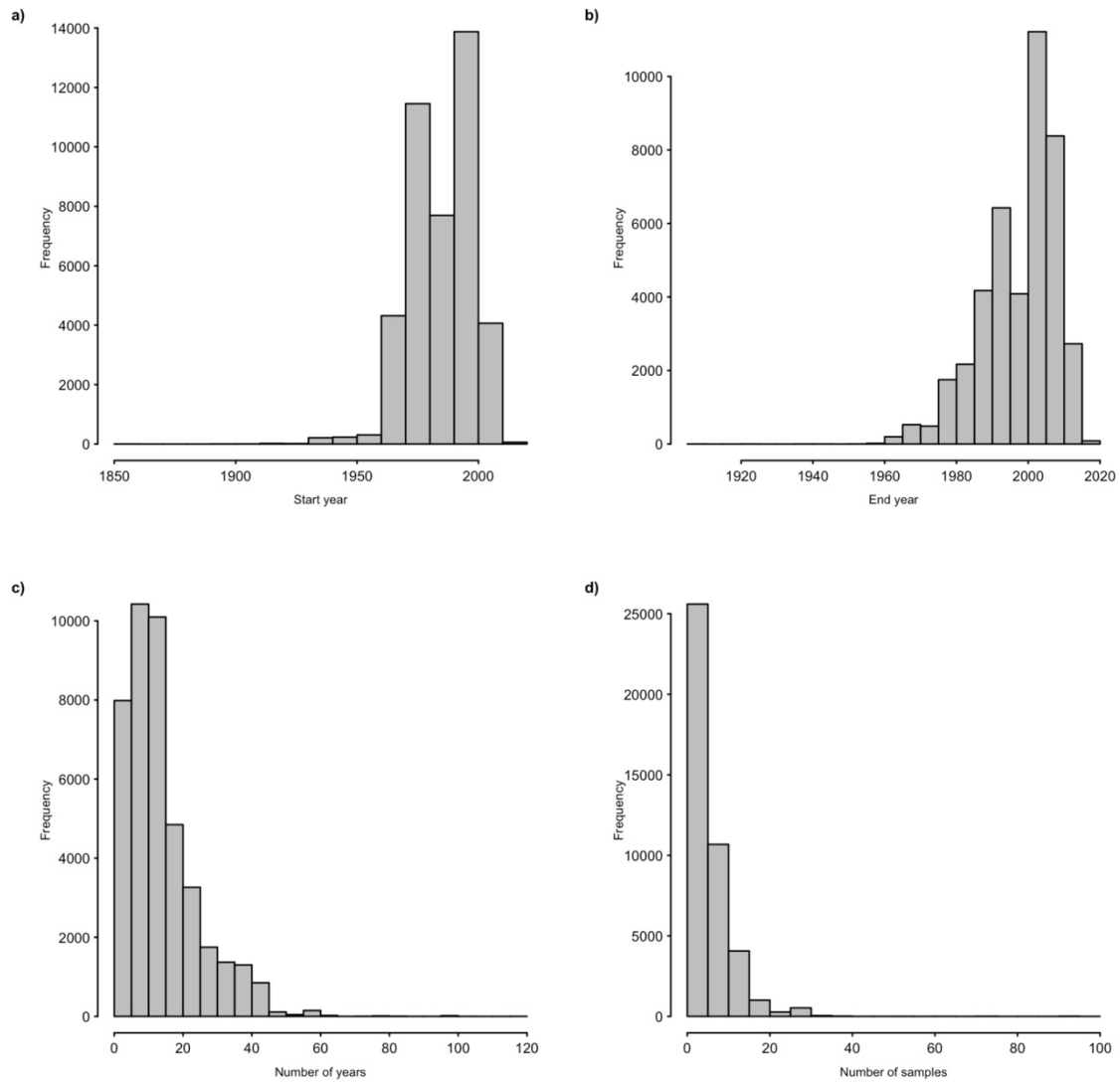
Competing interests:

Authors declare that they have no competing interests.

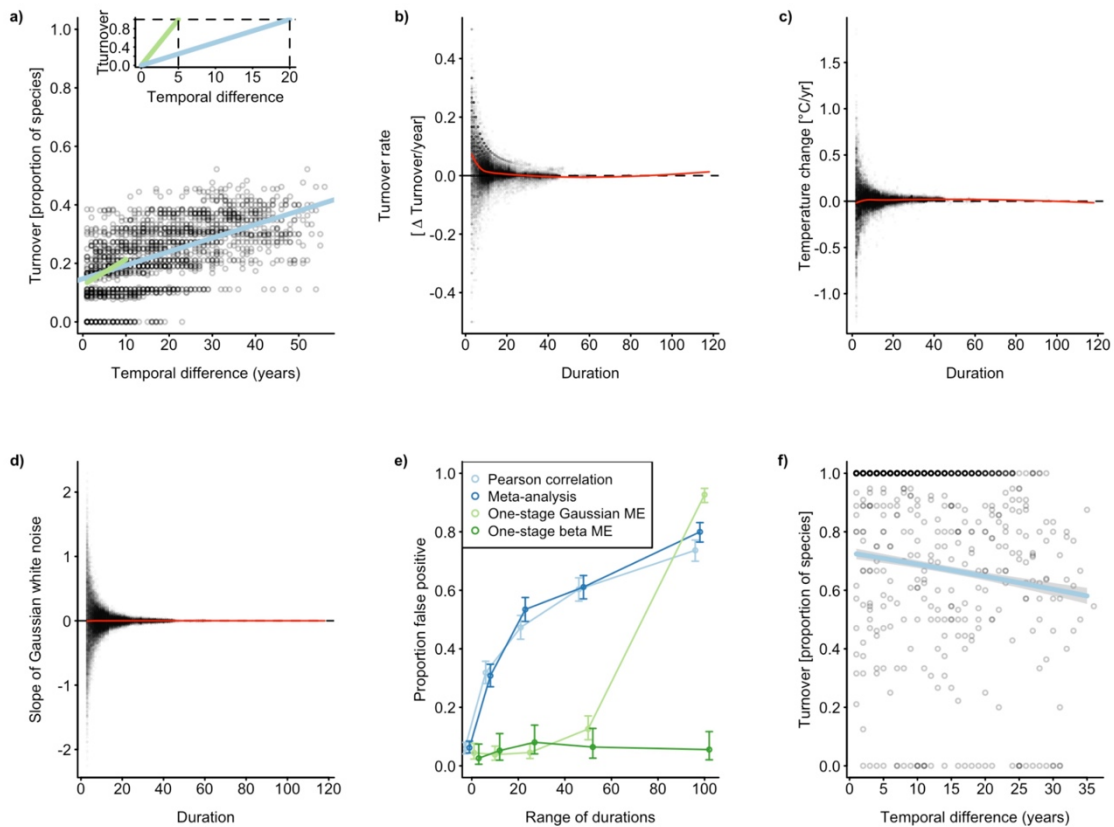
Additional Information:

Correspondence and requests for materials should be addressed to mpinsky@ucsc.edu.
Reprints and permissions information is available at www.nature.com/reprints.

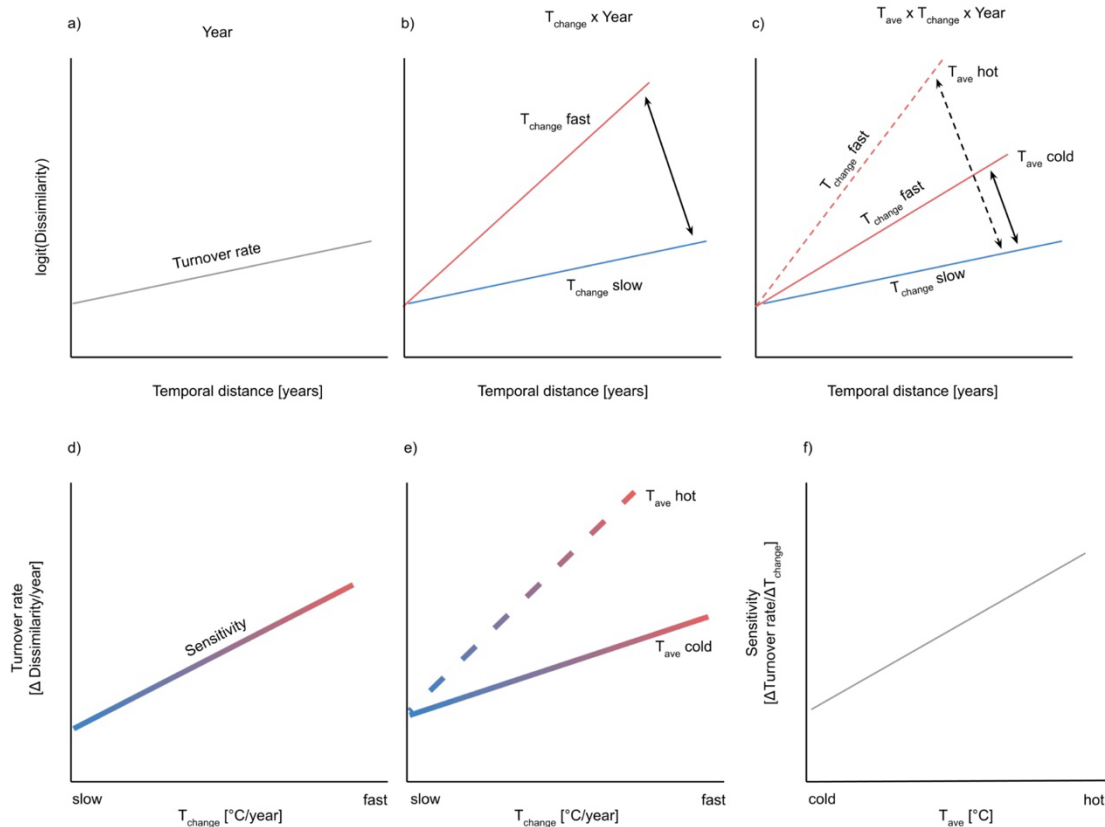
Extended Data Figures and Tables



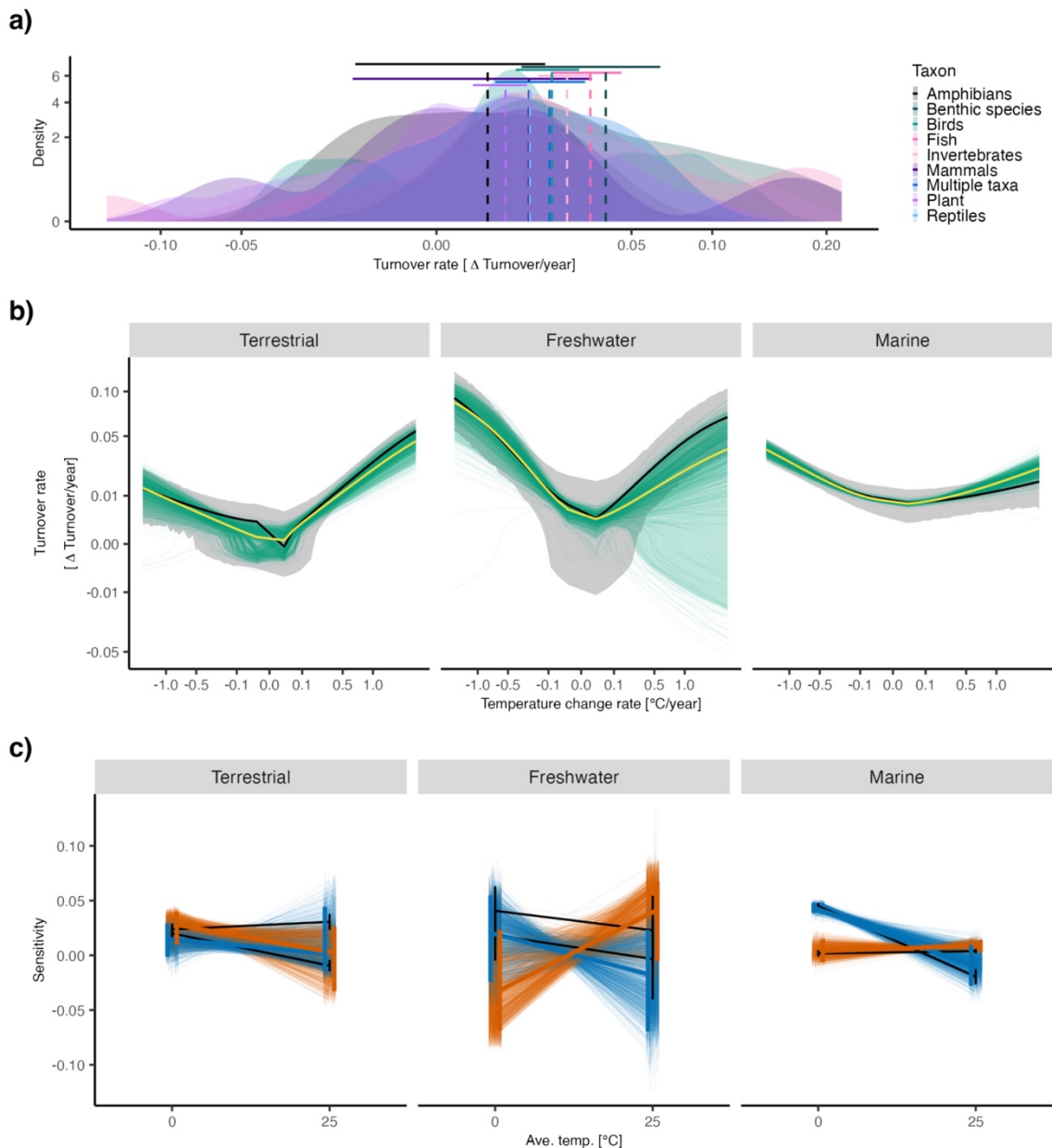
Extended Data Figure 1. Characteristics of the assemblage time series. a) Start year. b) End year. c) Number of years between the start and end year. d) Number of annual samples in each time series.



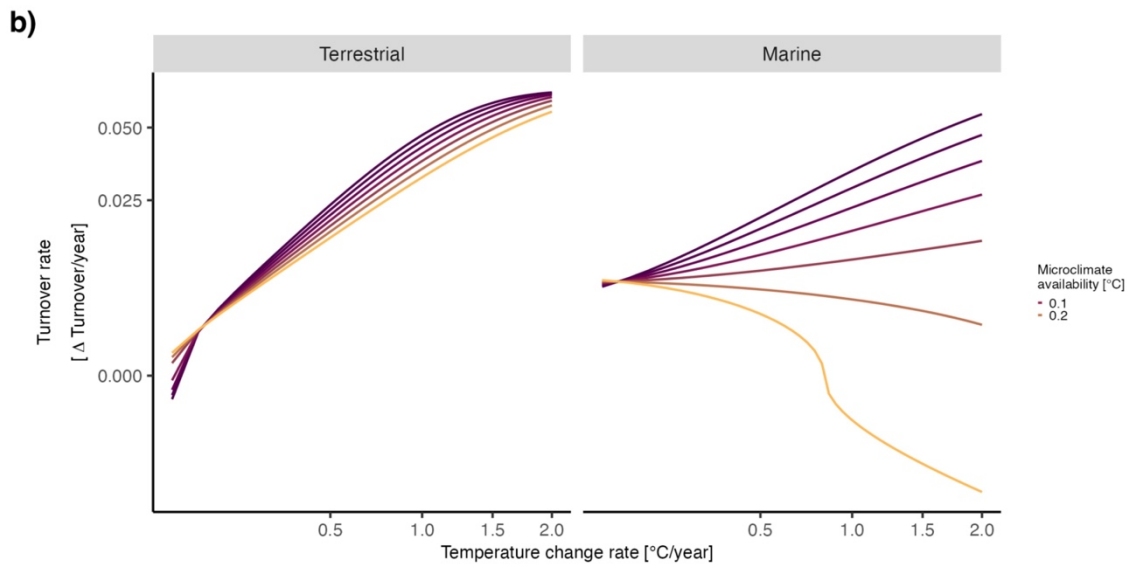
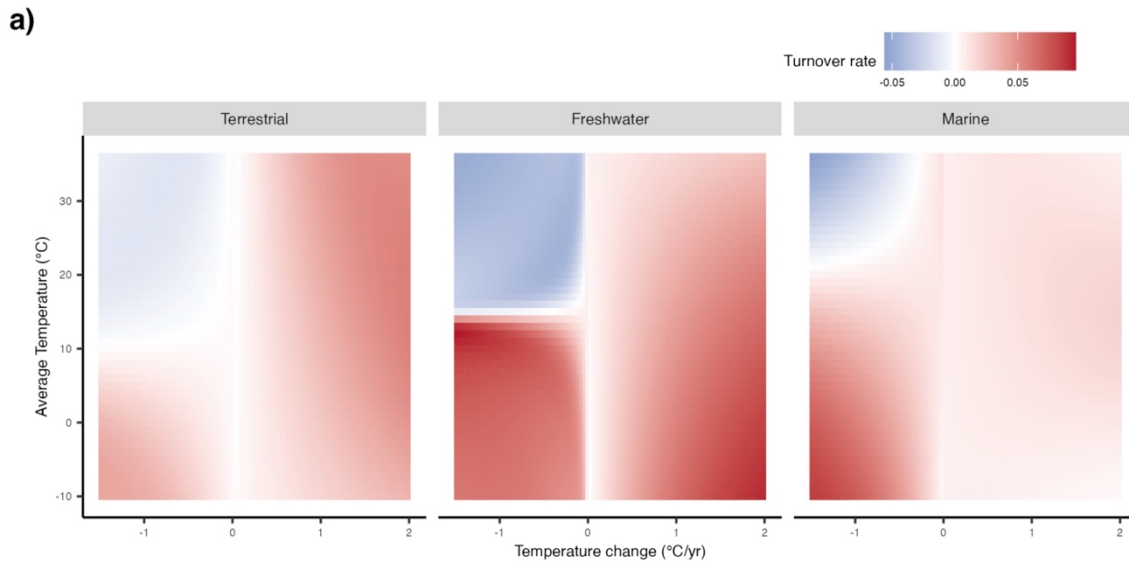
Extended Data Figure 2. The effect of time series duration on turnover rates (change in dissimilarity/yr) and the statistical challenges when time series are compared. a) Duration affects turnover rates partly because there is a 0-1 constraint on dissimilarity, such that longer duration time series (blue) are constrained to a shallower slope than shorter duration time series (green). b) Turnover rates show strong heteroskedasticity with higher variance and faster rates among shorter time series. The red line shows mean turnover rate estimated from LOESS smoothing. c) Temperature changes ($^{\circ}\text{C}/\text{yr}$) also showed strong heteroskedasticity with higher variance among shorter time series. The red line shows a fit from LOESS smoothing. d) Slopes calculated from Gaussian white noise time series also show strong heteroskedasticity with higher variance among shorter time series. The durations of the white noise time series matched the durations in the species composition dataset. The red line shows a fit from LOESS smoothing. e) A comparison of Type I (false positive) error rates shows that one-stage (i.e. fit directly to dissimilarities) generalized linear mixed models (GLMMs) with ordered beta errors have an acceptably low false positive rate when time series of different durations are analyzed together, while other common analytical methods (Pearson correlations of time series slopes, meta-analysis of time series slopes, or one-stage mixed effect models with Gaussian errors fit to time series data) have unacceptably high false positive rates if time series differ in duration (range of durations > 0). All methods have low false positive rates when time series are all the same duration (range of durations = 0). Data are presented as means with error bars for the 95% binomial confidence bounds. f) Example of a time series with a negative turnover rate. Data are demersal marine taxa from the Northeast Fisheries Science Center Bottom Trawl Survey. Beta regression trend line is shown with shading for \pm one standard error.



Extended Data Figure 3. The statistical approach was implemented via one-stage generalized linear mixed models (GLMMs) in which the response variable was species composition dissimilarity among years. a) The simplest model included the relationship between dissimilarity and temporal distance among observations so that, for example, dissimilarity could increase with time. The slope of this relationship is the turnover rate. Random intercepts and slopes helped account for variation among studies and time series (not shown). b) We tested the hypothesis that faster rates of temperature change (T_{change}) were associated with faster accumulation of dissimilarity through time (compare red vs. blue line). This hypothesis was statistically tested as an interaction ($T_{change} \times Years$). c) We additionally tested the hypothesis that the influence of temperature change on the turnover rate depended on average baseline temperatures. For example, the slope of dissimilarity over time could be steeper in areas with hotter average temperatures and fast rates of temperature change than in areas with colder average temperatures and fast rates of temperature change (compare dashed red vs. solid red line). Statistically, this was tested as a three-way interaction ($T_{change} \times T_{ave} \times Years$). d) Turnover rates as a function of temperature change rates, showing an increase in turnover rate with increasing rates of temperature change (i.e., the same relationship as panel b but summarized as rates). The slope of this relationship was termed sensitivity (Δ turnover rate/ Δ temperature change rate). e) Turnover rates as a function of temperature change rates and average baseline temperatures, showing a faster increase in turnover rate with temperature change at hotter average baseline temperatures (i.e., summarizing the same relationship as panel c). f) Sensitivity as a function of average temperatures, showing an increase in sensitivity at hotter average temperatures (i.e., summarizing the same relationship as in panels c and e). The x-axis could also be other environmental covariates, such as microclimates or non-climate human impacts (as in Figure 3).



Extended Data Figure 4. Association of turnover rate with taxonomic group and uncertainty of the association with temperature change and average temperature. a) Turnover rate [proportion of species per year] for studies organized by taxonomic group. Dashed lines are the averages across studies within taxa, and the top horizontal lines indicate the 95% confidence intervals on the averages. The x- and y-axes have been square-root transformed to facilitate visualization. b) Uncertainty in the marginal effects of temperature change on the turnover rate, calculated by downsampling each time series of dissimilarities (see Methods). Plot shows the individual downsampling effects (thin green lines), the average across 1000 downsampling trials (yellow line), the 95% confidence interval from downsampling (green shading), and the mean marginal effects from the full dataset with 95% confidence intervals (black line and shading). c) Uncertainty in the marginal effects of average temperature on the sensitivity of turnover rate to temperature change, calculated by downsampling each time series of dissimilarities (see Methods). Plot shows the individual downsampling effects (thin lines), the average across 1000 downsampling trials (thick lines), and the 95% confidence interval from downsampling (vertical error bars) for warming (orange) and cooling (blue). The mean marginal effects from the full dataset with 95% confidence intervals are also shown (black lines and error bars).



Extended Data Figure 5. Turnover rate model interactions. a) Interaction of T_{change} (x-axis) with T_{ave} (y-axis) from the $T_{\text{change}} \times T_{\text{ave}} \times \text{Year} \times \text{Realm}$ model (Table 1). Two average temperature levels (0 °C and 25 °C) from this interaction are plotted in Fig. 2c. b) Marginal effects of temperature change on the turnover rate (lines) as predicted from the best environmental interaction model identified by AIC (Extended Data Table 5). The model included effects of microclimate availability (colors).

Random effect	Std. Dev.	Correlation of slope & intercept
Time series ID intercept	0.362	-0.042
Time series ID Years slope	0.0252	
Study ID intercept	0.797	0.801
Study ID Years slope	0.0529	

Extended Data Table 1. Random effect standard deviations and correlations for the $T_{\text{change}} \times T_{\text{ave}} \times \text{Year} \times \text{Realm}$ model (see Table 1).

Realm	T _{change} sign	Term	Estimate	Std. Error	z value	p
Freshwater (baseline)		Intercept	-1.4	0.21	-6.5	6.8×10 ⁻¹¹
		D _{nit}	2.5	0.016	160	0
		Year	0.079	0.015	5.2	1.9×10 ⁻⁷
		T _{ave}	-0.13	0.14	-0.92	0.36
	cooling	T _{change}	-0.063	0.034	-1.8	0.067
	(baseline)	D _{nit} × Year	-0.09	0.0016	-56	0
		T _{change} × T _{ave}	0.082	0.098	0.84	0.4
		T _{ave} × Year	-0.024	0.016	-1.5	0.13
		T _{change} × Year	0.018	0.007	2.6	0.0086
		T _{change} × T _{ave} × Year	-0.049	0.021	-2.3	0.019
		Intercept	0.11	0.074	1.4	0.15
		T _{ave}	0.097	0.16	0.59	0.56
		T _{change}	0.04	0.04	1	0.32
	warming	Year	-0.02	0.0074	-2.8	0.0057
	T _{change} × T _{ave}	-0.075	0.11	-0.69	0.49	
	T _{ave} × Year	0.027	0.018	1.5	0.13	
	T _{change} × Year	-0.01	0.0087	-1.2	0.24	
	T _{change} × T _{ave} × Year	0.047	0.023	2.1	0.037	
Marine		Intercept	0.091	0.22	0.41	0.68
		T _{ave}	0.23	0.14	1.6	0.11
		T _{change}	0.048	0.034	1.4	0.17
		Year	0.0018	0.016	0.11	0.91
	cooling	T _{change} × T _{ave}	-0.076	0.099	-0.77	0.44
	(baseline)	T _{ave} × Year	0.029	0.016	1.8	0.073
		T _{change} × Year	-0.015	0.0071	-2.1	0.037
		T _{change} × T _{ave} × Year	0.046	0.021	2.2	0.03
		Intercept	-0.12	0.074	-1.6	0.1
		T _{ave}	-0.092	0.16	-0.56	0.58
		T _{change}	-0.027	0.041	-0.66	0.51
		Year	0.012	0.0074	1.6	0.11
	warming	T _{change} × T _{ave}	0.079	0.11	0.72	0.47
		T _{ave} × Year	-0.031	0.018	-1.7	0.081
	T _{change} × Year	0.0078	0.0088	0.88	0.38	
	T _{change} × T _{ave} × Year	-0.044	0.023	-1.9	0.055	
Terrestrial		Intercept	-0.43	0.22	-2	0.05
		T _{ave}	0.12	0.15	0.8	0.43
		T _{change}	0.051	0.035	1.5	0.14
		Year	-0.026	0.017	-1.5	0.12
	cooling	T _{change} × T _{ave}	-0.09	0.099	-0.91	0.36
	(baseline)	T _{ave} × Year	0.022	0.017	1.3	0.18
		T _{change} × Year	-0.019	0.0076	-2.6	0.01
		T _{change} × T _{ave} × Year	0.047	0.021	2.2	0.027
		Intercept	-0.12	0.083	-1.4	0.15
		T _{ave}	-0.14	0.17	-0.86	0.39
		T _{change}	-0.036	0.042	-0.86	0.39
		Year	0.013	0.0085	1.5	0.13
	warming	T _{change} × T _{ave}	0.087	0.11	0.8	0.43
		T _{ave} × Year	-0.026	0.018	-1.4	0.15
	T _{change} × Year	0.017	0.0094	1.8	0.074	
	T _{change} × T _{ave} × Year	-0.045	0.023	-1.9	0.053	

Extended Data Table 2. Fixed effect terms for the T_{change} × T_{ave} × Year × Realm model (see Table 1). Z values and p-values are from Wald tests. The marine, terrestrial, and warming effects are differences from the baseline values (Freshwater cooling).

Type	Model	df	AIC	Δ AIC	Δ AIC _{null}
Gain-loss	Year	18	770215	7524	0
	Realm × Year	20	770213	7523	-1.62
	Taxon × Year	32	770236	7545	21
	T _{change} × Year × Realm	38	769527	6837	-688
	T_{change} × T_{ave} × Year × Realm	62	762690	0	-7524
≥7 years	Year	17	645558	637	0
	Realm × Year	19	645550	629	-8.05
	Taxon × Year	31	645565	643	6.52
	T _{change} × Year × Realm	37	645421	499	-137
	T_{change} × T_{ave} × Year × Realm	61	644921	0	-637

Extended Data Table 3. As for Table 1, but models either 1) included an additional term for the interaction of initial dissimilarity (D_{init}), the proportion of species gains vs. losses ($propGL$), and the duration between observations ($Years$), and only included random effects for study, or 2) were fit to only time series with at least 7 years of data.

Model	df	AIC	Δ AIC	Δ AIC _{null}
Year	17	-461437	1231	0
Realm \times Year	19	-461434	1234	3.04
Taxon \times Year	31	-461419	1248	17.4
(T_{change} + Year) \times Realm	28	-461481	1187	-43.9
T_{change} \times Year \times Realm	37	-461633	1035	-196
(T_{change} + T_{ave}) \times Year \times Realm	43	-462327	341	-890
T_{change} \times T_{ave} \times Year \times Realm	61	-462668	0	-1231

Extended Data Table 4. Comparison of models of temporal turnover calculated with abundance-based Morisita-Horn dissimilarities with or without the temperature change (T_{change}) and average temperature (T_{ave}). Details as in Table 1. The most parsimonious model (highlighted in bold) included both T_{change} and T_{ave} .

	Model	df	AIC	ΔAIC_{temp}	ΔAIC_{null}
1	Year	15	669151	746	0
2	$T_{change} \times T_{ave} \times Year \times Realm$	44	668404	0	-746
3	Micro $\times T_{change} \times Year \times Realm$ + $T_{change} \times T_{ave} \times Year \times Realm$	52	668374	-30.8	-777
4	Human $\times T_{change} \times Year \times Realm$ + $T_{change} \times T_{ave} \times Year \times Realm$	52	668386	-18.1	-764

Extended Data Table 5. Comparison of models of temporal turnover with or without environmental covariates. Models with microclimate variability (#3, Micro) or human impact (#4, Human) were favored over the simplest Year model (#1) with dissimilarity as a function of year, shown as negative ΔAIC_{null} and were also favored over a model with only temperature (#2), shown as negative ΔAIC_{temp} . Columns show the degrees of freedom (df), Akaike's Information Criterion (AIC) compared to the AIC of the model with only temperature (ΔAIC_{temp}), and AIC compared to the null model (ΔAIC_{null}). The favored model is shown in bold.